# A Simulation Tool to Predict the Impact of Soil Topologies on Coupling Between a Light Rail System and Buried Third-Party Infrastructure

Charalambos A. Charalambous, *Member, IEEE*, Ian Cotton, *Senior Member, IEEE*, and Pete Aylott

***Abstract*—The production of stray currents by dc light rail systems leads to the corrosion of the supporting and third-party infrastructure in close proximity to the rail system. This paper simulates two parallel tracks that are occupied by two trains: one on each track. This type of modeling constitutes a case study that is utilized to investigate the effect of soil topologies on the corrosion performance of a floating dc light rail system focusing on the supporting and third-party infrastructure. The modeling technique used involves the accurate computation of the shunt and series parameters for use in a resistive-type model using a commercially available software package. The results demonstrate the importance that soil resistivity has on the corrosion risk to traction system and third-party infrastructure. Such information could ultimately be used to vary the level of stray current protection across a light rail system to ensure a consistent lifetime across the whole system.**

***Index Terms*—Corrosion, dc light rail, soil topologies, stray current.**

## I. Introduction

CURRENT leakage from dc railway systems is an inevitable consequence of the use of the running rails as a mechanical support/guide way and as the return circuit for the traction supply current. Since the rails have a finite longitudinal, or series, resistance (around 40–80 $\mathrm{m}\Omega/\mathrm{km}$ or 40–80 $\mu\Omega/\mathrm{m}$ of rail) and a poor insulation from earth (typically from 2 to 100 $\Omega$km), a proportion of the traction current returning along them will leak to earth and flow along parallel circuits (either directly through the soil or through buried conductors) before returning onto the rail and the negative terminal of the dc rectifier.

Given that the current flow in a metallic conductor is electronic, whereas that through electrolytes such as the earth, concrete, etc., is ionic, it follows that there must be an electron-to-ion transfer as the current leaves the rails to the earth. Where the current leaves the rail to earth, and an anode is produced, there will, therefore, be an oxidation, or electron-producing, reaction.

Manuscript received September 29, 2006; revised July 27, 2007, September 10, 2007, and September 11, 2007. The review of this paper was coordinated by Mr. D. Diallo.

C. A. Charalambous is with the National Grid High Voltage Research Center, The University of Manchester, M60 1QD Manchester, U.K. (e-mail: charalambos.charalambous@manchester.ac.uk).

I. Cotton is with the School of Electrical and Electronic Engineering, The University of Manchester, M60 1QD Manchester, U.K. (e-mail: ian.cotton@manchester.ac.uk).

P. Aylott is with CAPCIS Ltd., M1 7DP Manchester, U.K.

Color versions of one or more of the figures in this paper are available online at http://ieeexplore.ieee.org.

Digital Object Identifier 10.1109/TVT.2007.909312

The corrosion of metallic objects will, therefore, occur from each point that current transfers from a metallic conductor, such as a reinforcement bar in concrete, to the electrolyte (i.e., the concrete). Hence, the stray current leakage can cause corrosion damage to both the rails and any other surrounding metallic elements.

A key factor in determining the level of threat to the third-party infrastructure (utilities) and the supporting infrastructure is the resistivity of the surrounding soil. Typically, a uniform soil resistivity model is assumed over the length of a system. In reality, it will change with both depth and system chainage.

This paper builds on a previous work carried out in [1]–[3]. It describes a simulation tool that can be used to predict the level of stray current (and hence corrosion damage) in a dc light rail system, where the soil resistivity varies in the manner described above. In certain situations where the soil resistivity changes with depth, the buried utilities can experience significant protection from the stray current. However, a sudden change in soil resistivity along the length of the system can concentrate corrosion on a specific location. In such a case, protective measures may be specified at such a location to ensure the system lifetime is not compromised.

The simulation tool accurately calculates the current distribution between the rail, the stray current collection mat, and the buried utility. The modeling technique is demonstrated with a model of two parallel tracks that are occupied by two trains, one on each track. This type of modeling constitutes a realistic case study that can be utilized to investigate the stray current performance of a dc light rail system. Dynamic modeling, as well as static modeling, is possible with this technique. True visualization of the impact of the different soil models on the amount of corrosion seen on the transit system and the surrounding infrastructure is only possible using dynamic models. These dynamic models are essentially time-stepped static models in which the train position and velocity vary as a function of distance.

Since there is a tendency in new transit systems to utilize floating running rails (literature stating that floating running rails are the best option if the stray current is to be minimized [3]–[5]), this paper specifically addresses the corrosion performance of floating dc light rail systems. However, the simulation tool does have the capability to incorporate solidly bonded and diode-bonded systems [6], [8].

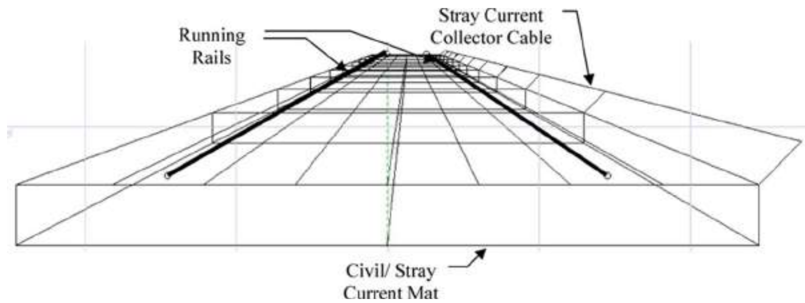


Fig. 1. Geometrically accurate CDEGS model in perspective view.

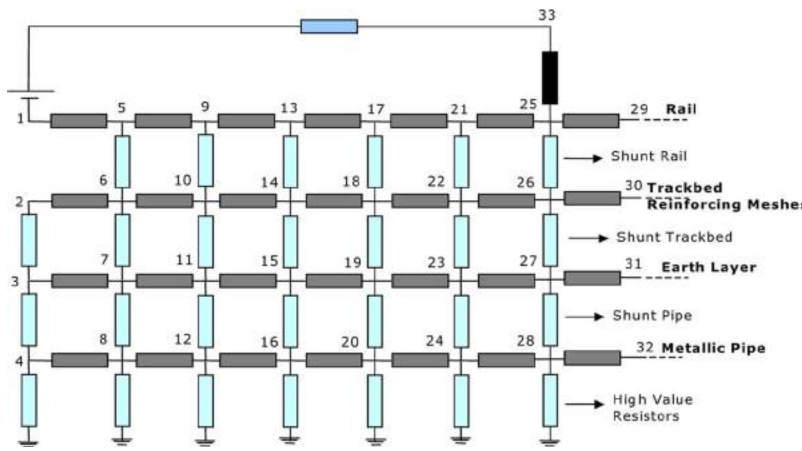


Fig. 2. Resistive network for the rail, track bed, and metallic pipe (floating system).

## II. Model System

### A. Introductory Remarks

The essential elements of a transit system are the rails, the rail-to-earth insulation, the power supply, and the vehicles. The design and placement of these elements of the transit system dictate the stray current performance in terms of the total stray current leaving the rails [1], [3].

The work carried out in [1] described the design principles employed in current distribution, electromagnetic fields, grounding, and soil structure analysis (CDEGS) [7] to accurately model the current distribution between structures of a dc light rail system by taking into consideration the geometry of the system, the soil topology, and the interactions between the metallic structures under study. Fig. 1 illustrates the perspective view of the CDEGS model, for the rails, their supporting infrastructure (track bed), and a third-party infrastructure (e.g., buried metallic pipe).

The work carried out in [2] described a simulation tool that is a two-step process combining the accuracy of CDEGS with the flexibility of a resistive network model implemented in MATLAB. CDEGS is initially used to investigate the self and mutual resistances of metallic structures in various soil structures, taking into consideration factors like buried depth, material of conductor, coating, radius, length, and geometrical arrangement.

The reinforced concrete mat placed underneath the rails is used for both structural support and as a conductive path for the stray current. Connected to this mat is an insulated cable (generally copper) that increases the overall conductivity of the stray current collection circuit relative to the alternative stray current paths in the soil and other buried objects. The CDEGS model effectively calculates a combined resistance parameter for both the track-bed reinforcing bars and the connected collector cable.

The information provided by CDEGS is then appropriately employed in a simplified resistive network that speeds up the simulation time while, at the same time, maintains the accuracy of the results produced. This form of model has a number of advantages, one of them being the fact that it can be dynamically utilized to acquire a true visualization of the stray current corrosion risk. Fig. 2 illustrates the resistive-type network. The components of this model are described in more detail in the next section of this paper.

### B. Description of Static Simulation Model

The described model has been further enhanced to simulate two parallel tracks that are occupied by two trains, one on each track. With this form of modeling, parameters such as the effect of cross bonding the tracks on the stray current level produced by the system can be examined. In dc-electrified railways, it is a common practice for the rails of each track to be bonded together and for the tracks to be cross bonded to reduce the resistance of the return path, thus reducing the generation of stray currents.

As in previous modeling efforts, geometrically accurate models are first built in the software. These models, as shown in Fig. 3, are relatively short in length owing to the high complexity of the model. They are used to develop and validate

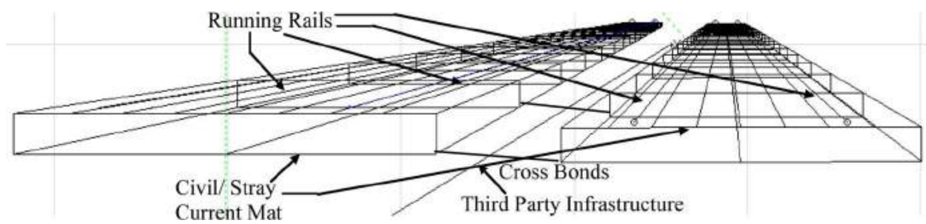


Fig. 3. Geometrically accurate CDEGS model for two tracks in perspective view.

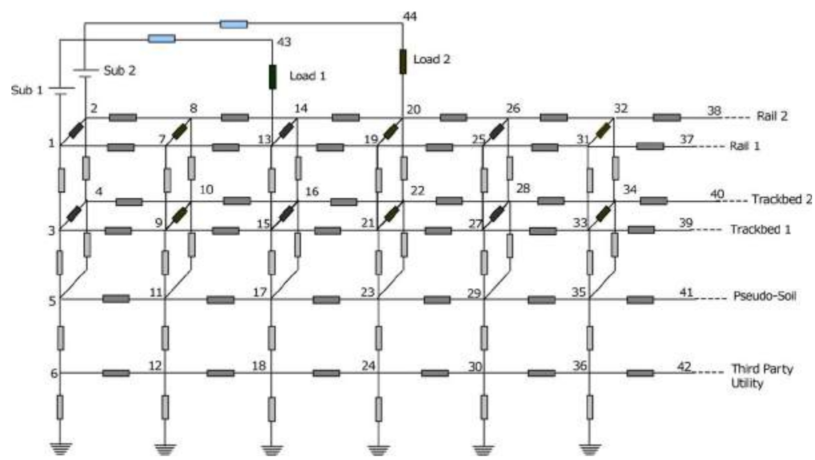


Fig. 4. Resistive-type network for the double-track floating system.

[8] the resistive-type network shown in Fig. 4. If changes in soil resistivity occur over a system length, multiple models would be run to produce different resistive network parameters for each individual case.

The resistive network that has been produced is shown in Fig. 4 and includes (at the top) two sets of resistors that represent the two tracks. For modeling purposes, the equivalent series resistance of each track is represented by one resistor layer based on the assumption that only one rail is used for the return current (the other is used for signaling).

A shunt resistor then represents the resistance of the rail to the track bed (in reality, this is practically the same as the resistance to earth of the rail for most well-coated systems). Below each set of the resistors representing the rails, there also exists a resistor layer that represents the equivalent series and shunt resistance of the track bed (stray current collection mat). Each track has its equivalent track bed situated beneath it.

The third layer is the "pseudo-earth layer," which can be appropriately modified for different soil structures. This layer is important to be included as it is recognized that some current flows through the earth and that this has a finite conductivity. This layer is placed before any third-party infrastructure, as current will always flow from the track bed into the earth before reaching such an infrastructure. The final fourth layer represents the series and shunt resistances of this third-party infrastructure/metallic pipe.

The series resistance of the rail, the metallic mat, and the buried pipe can easily be calculated using the cross-sectional area, length, and resistivity of each conductor's material. The series resistance of the pseudo-earth layer, which varies according to soil resistivity, is determined by an iterative process (the end result requiring the results from a resistive model to match that of the more complex CDEGS model).

Additionally, the resistive model includes four sets of shunt resistors that interconnect the different layers. The role of the shunt resistors in conjunction with the "pseudo-earth layer" is to provide the conductive path between the different structures; these values vary according to the specified soil structure. Of particular note is that the values of shunt resistance for the rail are determined by approximating the resistance of the insulating pads that support the rail on the track bed.

The values of shunt resistance used for the track bed and the metallic pipe are initially determined by CDEGS by determining the resistance to earth of each structure. Simple models (not time consuming) need to run in CDEGS to determine the resistance to earth, according to the specified soil environment.

The resistive model uses the produced database of resistance to earth values (depending on specified soil structures) and can employ those in every consecutive section when multiple soil models are present.

This does not, however, fully reflect the resistance between the individual elements, and the values of these are, therefore, iterated along with the series resistance of the pseudo-earth later to accurately reproduce the CDEGS current distribution in the resistive model.

Of all the parameters detailed in this paper, the value of the soil resistivity used is likely to introduce the greatest source of error into the modeling process. The CDEGS software has been shown to be accurate by many researchers around the world and has been extensively verified.

The models described in this paper are simplifications of a real system (for example, the track bed reinforcement bar would be too complex to allow the modeling of all conductors), but these simplifications were used after confirming that they did not cause an error in any expected current/voltage of more than 1% [1].

The error introduced by the soil resistivity relates to the fact that it is difficult to measure and that it changes as a function of the season/weather conditions. These statements can be qualified by work carried out by other researchers. Ma and Dawalibi state that the soil resistivity measurements can be in error by as much as 50% when measurements are taken in proximity to metallic buried structures [9]. For a new light rail system in an urban environment, it is highly unlikely that such buried structures will not be present.

Other researchers find that soil resistivities can change in a local environment by a factor of 20 according to the level of moisture present within the soil [10]. The soil near the earth boundary is likely to be significantly affected. It would, therefore, be prudent in any analysis to consider likely variations in soil resistivity over a year and the influence of buried objects on measurements before carrying out simulations.

The system that has been studied is modeled on the basis of the parameters given in Table I. Two tracks are modeled along with the track beds that are placed underneath them. The location of cross bonds can be controlled by the user and can be placed every 100 m, 200 m, 300 m, etc. In this case, the tracks are cross bonded every 100 m, as is the track bed itself. Cross bonds have been shown to be beneficial in controlling the levels of stray current on a floating dc light rail system [11].

It is noted that the model has the capability of modeling randomly spaced cross bonds. It is also possible not to include cross bonds (isolating the tracks by using high value resistors) or to randomly select which cross bonds are conducting. Consequently, the cases where the train locations do not coincide with the cross-bond locations can be investigated.

TABLE I
DESIGN PARAMETERS OF THE SIMULATION MODEL

| | | |
|---|---|---|
| RAILS | Series Resistance: | 0.04 Ω/km |
| | Resistance to earth: | 320 Ωkm |
| | Number of conductors: | 1 |
| | Buried at depth: | 0.05 m |
| METALLIC MATS | Series Resistance: | 0.08 Ω/km |
| | Resistivity of Coating: | 180 Ωm / thickness 40 mm |
| | Radius: | 0.0094 m |
| | Number of conductors: | 10 longitudinal |
| | Buried at depth: | 0.628 m |
| PIPES | Series Resistance: | 1.437 mΩ/km |
| | Radius: | Ext: 0.61 m Int: 0.512 m |
| | Number of conductors: | 1 hollow |
| | Buried at depth: | 20.628 m |
| CROSS BONDS | Series Resistance: | 1.437 mΩ |
| | Cross Sectional Area: | 120 $mm^2$ |
| | Number of conductors: | Every 100 m |
| | Length: | 10 m |
| POWER | Train current: | 1000 A |

## C. Validation of Static Simulation Model

As a starting point, the system is modeled in CDEGS. The capability of the software to select shunt and series parameters is utilized with the ultimate purpose of establishing an agreement between CDEGS and resistive network results in terms of the stray current distribution between the different metallic structures.

The models shown in Figs. 3 and 4 are implemented in MATLAB using the resistive model. Equivalent geometrically accurate systems were also developed in CDEGS. All of the models used in this section relate to systems placed in a soil resistivity of 100 Ωm. Validations of the shunt/series parameters used later in this paper for the alternative soil models have been carried out but are not presented.

The first case study (i.e., Fig. 5) illustrates a 1-km section of two parallel tracks, which represent the geometrically accurate CDEGS model of Fig. 3. These 1-km sections are representative of a symmetrical 2-km section of two parallel tracks with two trains at the center of each track and a substation at the same end of each track, drawing a constant current of 1000 A each.

This static model assumes worst-load conditions; it thus constitutes a worst-case scenario for modeling the impact of stray current on the rails, the track bed, and the third-party utility structure. It is, however, noted that for a double-end feeding situation, more trains in the section will result in more current demands and, hence, greater leakage current. The so-called worst-case scenario, when considering a single train fed from one substation, is just a quick preliminary crude assessment for the stray current performance, and this is how it is perceived by the authors.

Figs. 6 and 7 illustrate a comparison of the results obtained by CDEGS simulations using the static models presented in Fig. 3 and by simulation of the resistive-type network (Fig. 5) in the case where the tracks are cross bonded. The graphs show the net current leakage profiles of the stray current collection mat (track bed) and the third-party utility.

The net current leakage is taken to be the difference between the stray current entering the structure and that leaving the structure (for example, on a track bed, the current may enter at the top of the track bed, some will then exit at the base, and the remainder being carried along the track bed). The maximum difference between the results from the MATLAB resistive model and those obtained by CDEGS is 2.2%.

The results are those expected when a floating rail system is simulated, i.e., one half of the system shows current flowing into the metallic conductors, whereas the other half of the system shows current leaving the conductors.

The second case study in Fig. 8 considers the same basic model used in case study I but has the position of the load

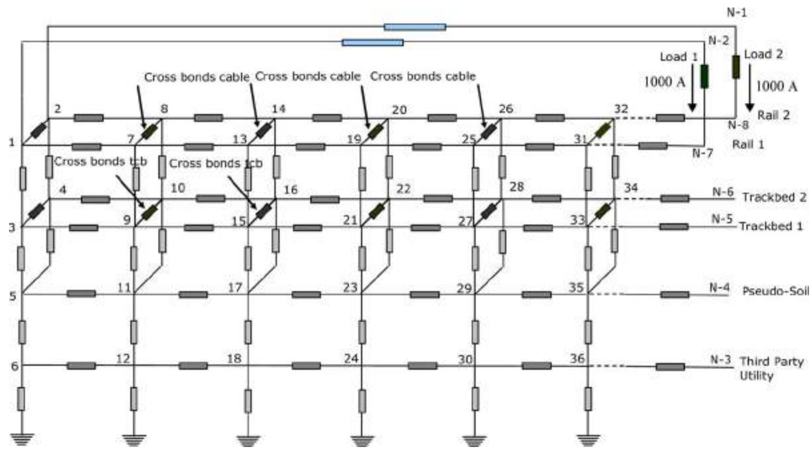


Fig. 5. Resistive-type network, substations same end (case study I).

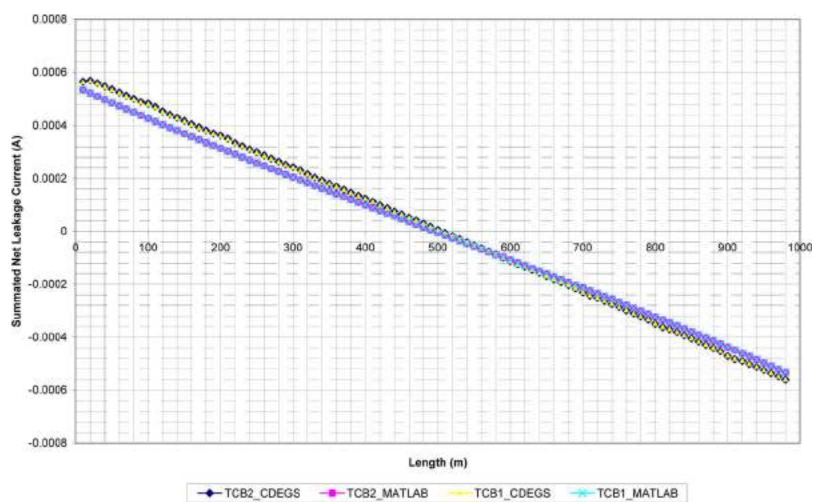


Fig. 6. Summated net current leakage of track beds obtained by CDEGS and MATLAB with the tracks cross bonded (case study I).

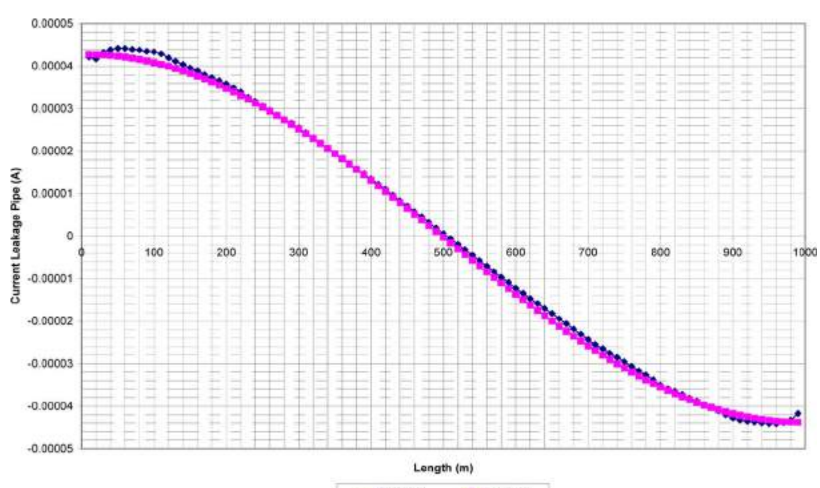


Fig. 7. Summated net current leakage of the third-party utility obtained by CDEGS and MATLAB with the tracks cross bonded (case study I).

(train) and the substation swapped on one of the tracks. The objective of this case study is to demonstrate the effect of substation placement on the stray current level of the rails and the third-party infrastructures in addition to the effect of cross bonding the two tracks. The values of the shunt parameters in the resistive network of Fig. 8 have not been altered and are the same as those employed in the case study in Fig. 5.

Figs. 9 and 10 illustrate a comparison of the results obtained by CDEGS simulations using the models presented in Fig. 3 (the direction of currents is reversed to cope with the change

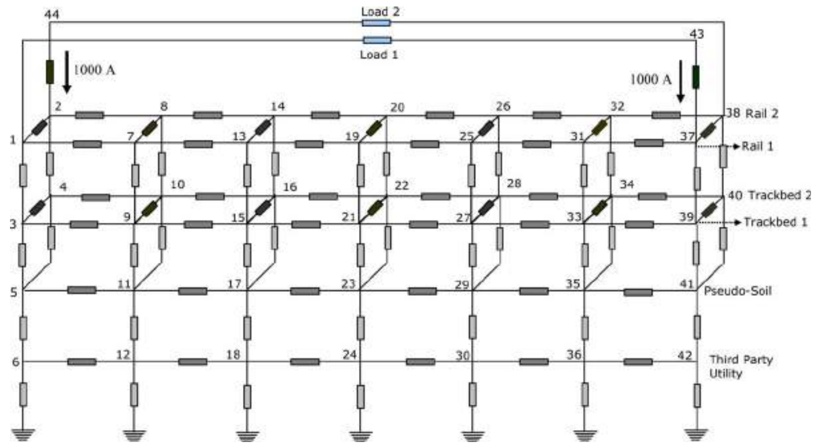


Fig. 8. Resistive-type network, substations opposite end (case study II).

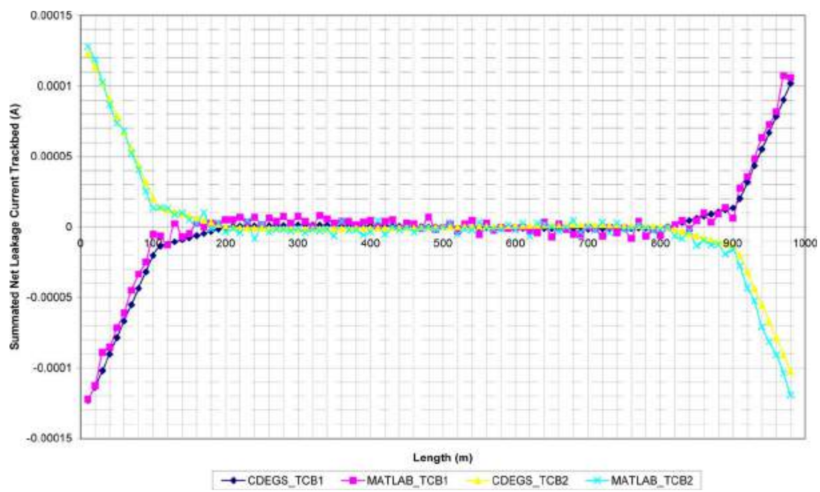


Fig. 9. Summated net current leakage of track beds obtained by CDEGS and MATLAB with the tracks cross bonded (case study II).

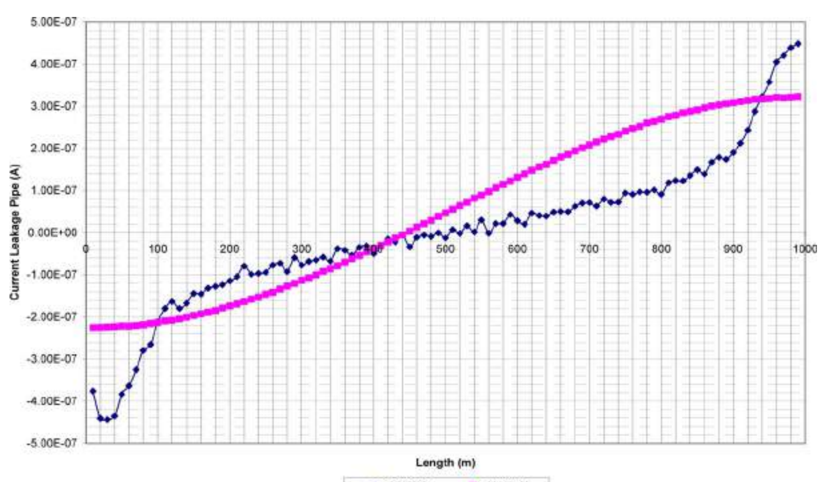


Fig. 10. Summated net current leakage of the third-party utility obtained by CDEGS and MATLAB with the tracks cross bonded (case study II).

of substation placement) and by simulation of the resistive-type network (Fig. 8).

The results presented in Fig. 9 show a good agreement between the MATLAB and CDEGS models, although the level of stray current is significantly less (a maximum value of just under 0.15 mA is observed, in comparison to 0.6 mA in the previous case). The reduction in the level of stray current relates to the flow of traction current in opposite directions and the ultimate cancellation due to the cross bonds connecting the two tracks. The stray current will not be reduced to zero, owing to the finite resistance of the track between the cross-bond locations and the resistance of the cross bonds themselves.

In the first case, a maximum current slightly lower than 0.5 $\mu$A is seen entering the pipe. In the second case, the simulations show an increased error between the MATLAB and CDEGS computations. However, in this case, the maximum current seen entering the pipe is less than 0.5 $\mu$A, according to CDEGS and just over 0.2 $\mu$A according to MATLAB. The discrepancy is attributed to the numerical error introduced into the CDEGS results by a matrix inversion process. The error introduced becomes significant at this level of current. However, this level of current is so small that it is not of concern when it is to be used to consider corrosion risk.

The fact that identical series and shunt resistance parameters (for the rails, the track beds, the earth layer, and the third-party utility structure) were employed in both resistive-type network models (Figs. 5 and 8) and that the results obtained from the developed algorithm in MATLAB and CDEGS modeling are consistent gives confidence in the validity of the proposed simulation tool.

The runtime simulation of the developed algorithm in MATLAB is dramatically reduced when compared with the runtime simulation that an equivalent model in CDEGS requires. This directly relates to the number of elements required to accurately simulate the system and, therefore, to the maximum system size that could be simulated as well (this being driven by memory capacity).

This reduction in the simulation runtime and enhancement of the system size that could be studied does not come at the expense of the accuracy of the results.

Table II tabulates the percentage of discrepancy in the current leakage profiles of the elements employed in this paper. The presented data are weighted averages of the discrepancies (CDEGS versus MATLAB values) of the current leakage along the entire length of each structure (total stray current). Additionally, the table provides a comparison of the computation time monitored for each model. The physical description of the models is given in Table III.

### *D. Investigation of the Effect of Alternative Soil Structures*

The purpose of this paper is to examine the impact of different soil structures on the stray current distribution. CDEGS allows the user to define the characteristics of the soil in which the conductors are being modeled. If the soil is not uniform, a layered soil model can be specified.

A maximum of three horizontal earth layers or three vertical earth layers may be specified in terms of their resistivity and layer thickness. CDEGS could, therefore, allow the construction of resistive models of systems placed in different soil environments. In terms of implementing this into the resistive model, a system that is considered to pass through three different soil resistivity regions would require three sets of shunt/series parameters from three different CDEGS simulations, all using the alternative soil resistivity values.

In this paper, simulations using uniform soils, two-layer horizontal soils, and two-layer vertical soil resistivity environments are presented, utilizing the resistive model simulation tool developed. Ultimately, the simulation tool can be utilized to formulate a soil structure with unlimited variations along the route [8]. Table III gives the specific details of the various models used in this paper.

The uniform soil models employed in this paper are representative of the soil structures, e.g., 10 Ωm corresponds to wet organic soil, 100 Ωm corresponds to moist soil, and 1000 Ωm corresponds to dry soil [12].

Uniform models A and B allow all of the systems to be enclosed by the same soil resistivity (although the rails remain coated by a high-resistivity layer to enable simulation of the correct rail-to-earth resistance and the track bed conductors are coated with a layer equivalent in thickness and resistivity to the cover provided by the track bed concrete).

In the case of the two-layer horizontal models, the rail and the track bed both lie in the top layer, whereas the metallic pipe lies in the bottom layer. The track bed and rail are placed into the same environment, as they are in close proximity to real dc light rail systems. The two simulated models represent the cases where the soil resistivity increases with depth (model C) and the case where the resistivity decreases with depth (model D).

For the two-layer vertical models, the rail, metallic mat, and pipe all see a change in soil resistivity at a distance of 500 m, i.e., half of their length lies in a high-resistivity soil, whereas the other half lies in a low-resistivity soil.

For the four-layer vertical models, the rail, metallic mat, and pipe all see a change in soil resistivity at a distance of 250 m, i.e., a quarter of their length lies in a 10-Ωm resistivity soil, a quarter of their length lies in a 100-Ωm resistivity soil, a quarter of their length lies in a 1000-Ωm resistivity soil, and the last quarter lies in a 10-Ωm resistivity soil.

## III. Dynamic Modeling

In this section, a simple dynamic model has been used in which a train is moved along a 1000-m section of track while drawing a constant current (to represent running at constant velocity on a constant gradient). The stray current assessment has been based on an equivalent effective traction current of 1000 A. The results may be scaled to other traction currents if desired, as this is a linear system.

By monitoring the total positive stray current (i.e., current leaking off a metallic structure) during each time step of the simulation, the total corrosive stray current can be obtained by its integration. This is defined as the gross leakage charge. The negative stray current, i.e., that returning onto structures, is not considered as this does not cause any corrosion to take place and does not reverse the corrosion process caused by a positive stray current leakage.

The simulation results presented in Section IV are based on a scenario in which two substations are placed at opposite ends of two tracks and in which the trains are moved in opposite directions, as illustrated in Fig. 11. The two tracks are cross bonded.

There is no particular significance in the choice of the system, and the results that have been obtained will, therefore, only serve to give conclusions that relate to the importance of the accurate simulation of soil structures.

TABLE II
PERCENTAGE OF DISCREPANCY TOTAL STRAY CURRENT ON METALLIC STRUCTURES: A COMPARISON BETWEEN CDEGS AND MATLAB

| | % Discrepancy in results CDEGS – MATLAB model | | | Computation Time (seconds) | |
|---|---|---|---|---|---|
| **Soil Structures** | **Rail** | **Trackbed** | **Metallic Pipe** | **CDEGS** | **MATLAB** |
| **Model A-Uniform** | 0.13 % | 1.69% | 2.08 % | 91.50 | 3.3 |
| **Model B-Uniform** | 0.36 % | 0.92% | 0.18% | 91.53 | 3.3 |
| **Model C-Horizontal** | 0.14% | 2% | 7.6% | 127.1 | 4 |
| **Model D- Horizontal** | 0.35% | 0.95% | 0.0318% | 205.35 | 4 |
| **Model E- Vertical** | 0.23% | 3.87% | 0.9% | 326.7 | 5 |

TABLE III
MODELS EMPLOYED IN SIMULATIONS

| | | |
|---|---|---|
| **UNIFORM MODEL** | | |
| Model A | 10 Ω.m | 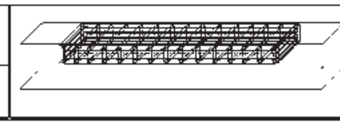 |
| Model B | 1000 Ω.m | |
| **TWO LAYER HORIZONTAL MODEL** | | |
| Model C | *Top Layer*:10 Ω.m /*Bottom Layer*:1000 Ω.m | 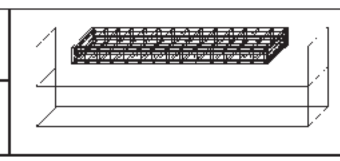 |
| Model D | *Top Layer*:1000Ω.m /*Bottom Layer*:10Ω.m | |
| **TWO LAYER VERTICAL MODEL** | | |
| Model E | *Front Layer*:10 Ω.m / *Back Layer*:1000 Ω.m | 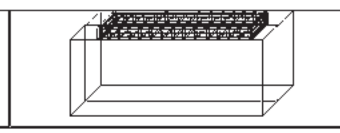 |
| **FOUR LAYER VERTICAL MODEL** | | |
| Model F | *A Layer*:10 Ω.m / *B Layer*:100 Ω.m/ C *Layer*:1000 Ω.m/ D *Layer*:10 Ω.m | 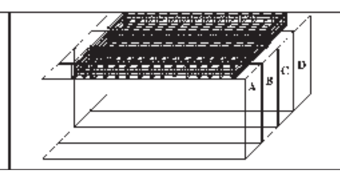 |

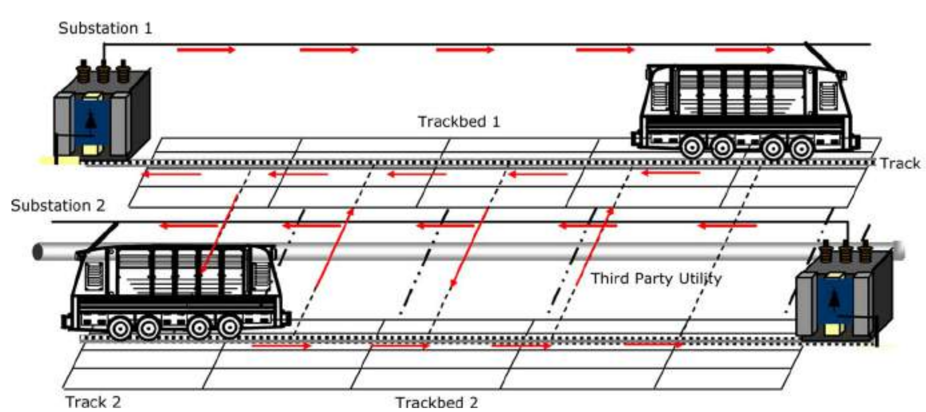


Fig. 11. Schematic arrangement of simulation model (substations opposite end).

Fig. 12 illustrates a flowchart of the operation of the software in terms of the calculation of the stray current distribution for each static model and the procedure that then determines the gross leakage charge of the rails, track beds, and third-party utility structure.

## IV. SIMULATION RESULTS

When the system is simulated with one movement of the trains, i.e., from one end of the track to the other (respectively), the gross leakage charge for all of the individual system elements can be described. The gross leakage charge of the rail

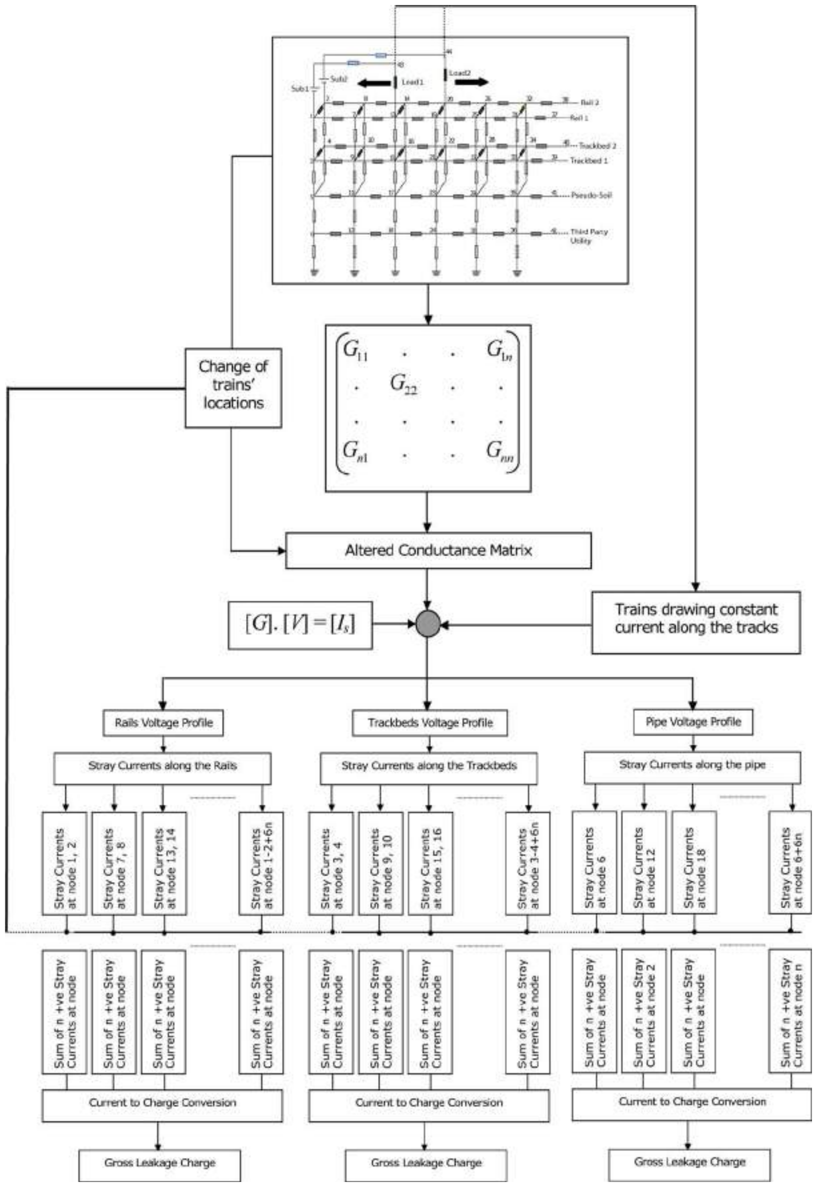


Fig. 12. Flow chart to determine the gross leakage charge.

is the same for all the soil resistivity models due to the high resistance of the coating layer placed along the rails. Fig. 13 illustrates the cumulative leakage charge profile for all three uniform model cases.

Fig. 14 illustrates the corrosive leakage charge of the base of the track bed for all soil resistivity models except F (this is used later in the paper). Only the base of the track bed is considered since the corrosion at the top of the track bed is assumed to be proportional to the rail leakage current (owing to the direction in which the current will flow into the track bed from the rails) and is, therefore, invariant as a function of soil resistivity.

Fig. 14 shows the significant impact of the vertical soil structure (model E) on the leakage current with a large discontinuity being present at the soil structure boundary. It is significant that in the lowest soil resistivity region (10 $\Omega$m at 0–500 m), the observed leakage currents are higher than those seen in soil model A, which has a uniform resistivity of 10 $\Omega$m.

When comparing models B and D, the performance of the track bed stays reasonably constant, although in D, the bottom layer resistivity has significantly decreased from 1000 to 10 $\Omega$m. The reason for the performance of the track bed staying reasonably constant is the high reflectivity factor at the boundary between the top and bottom soil layers. When the upper layer resistivity is large in comparison to the lower layer (as in model D), the reflection index is approximately 1, and the current cannot penetrate into the lower layer [9]. The current can, therefore, not easily reach the pipe or the lower resistivity and is retained on the track bed in a similar way as the 1000-$\Omega$m uniform soil model.

When comparing models A and C, the bottom layer resistivity increases from 10 to 1000 $\Omega$m, and the level of gross leakage charge on the base of the track bed is seen to significantly decrease [1].

Fig. 15 illustrates the cumulative corrosive leakage charge of the third-party utility structure (metallic pipe) for all the soil resistivity models (except F) tabulated in Table II.

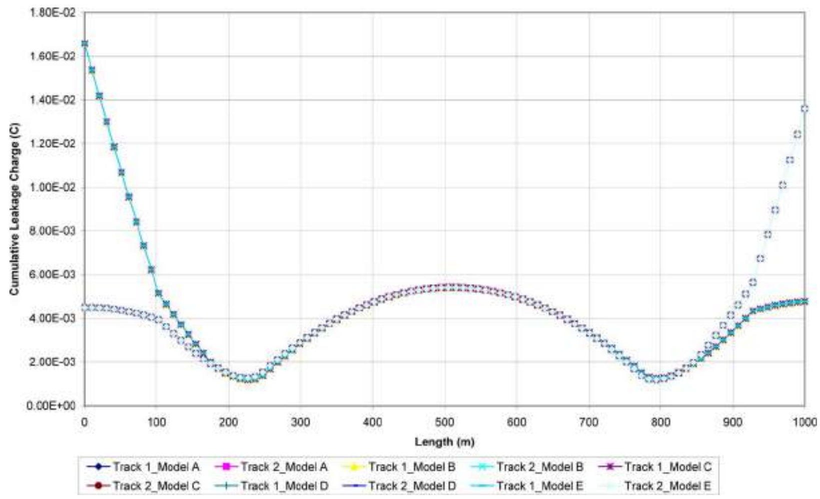


Fig. 13. Cumulative leakage charge rails.

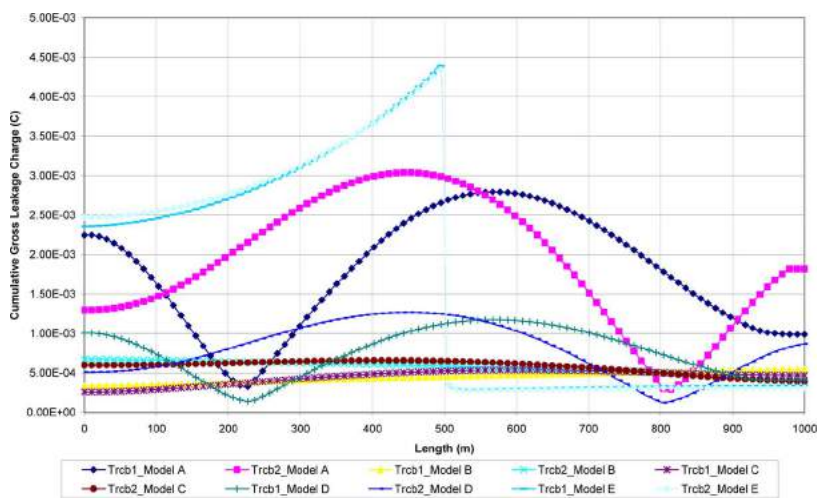


Fig. 14. Cumulative leakage charge base of the track beds.

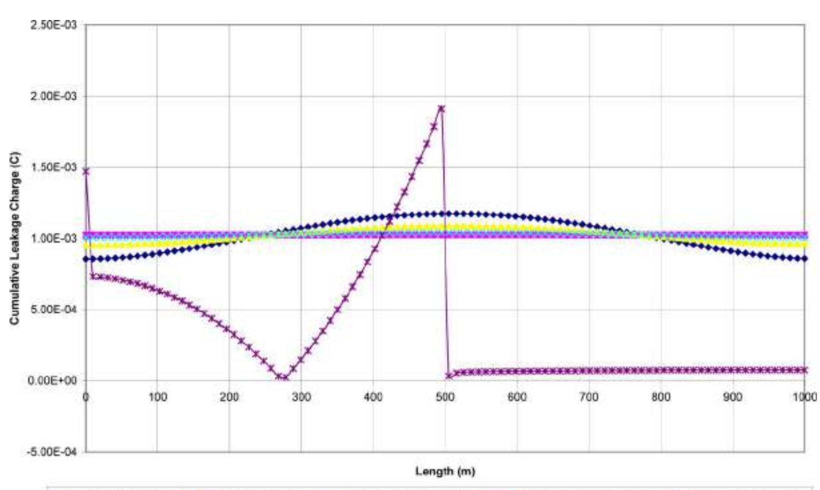


Fig. 15. Cumulative leakage charge of the third-party infrastructure.

The results for the vertical soil model E verify the previous conclusions [1], i.e., that a concentrated current leakage region will exist on the third-party utility structure and track bed when a vertical soil model exists. The discontinuities highlighted in Figs. 14 and 15 show that some portions of the system around the soil interfaces are more at risk.

The results shown in Fig. 15 also illustrate the fact that in homogenous systems, high soil resistivities mean that the third-party buried structures are less vulnerable to corrosion damage, whereas in low soil resistivities, the converse is true.

## V. Example of Modeling a Real System

This paper is intended to aid in the accurate modeling of real transit systems. This example of modeling utilizes Model F, which is a four-layer vertical soil structure, as illustrated in Table II. The details on the technique utilized to formulate a multilayer soil structure are given in [8]. An example of the use of modeling in the analysis of a simple system is now presented.

The model consists of two 1-km tracks, as shown in Fig. 11, on which the trains move with a constant velocity in opposite directions and, hence, draw a constant current. The current used in this simulation is 1000 A. The results could be linearly scaled for other values of current.

The operational condition is that the trains move along the section of track with a headway of 3 min. This will result in 20 trains running per hour on each track (therefore, 40 trains per hour on both tracks). Assuming that services are running for 19 h, i.e., from 5 A.M. until midnight, the total number of trains that will run across the section of two tracks under study would be 760. Therefore, the total charge produced by the movement of 760 trains will be 760 times more than the charge produced by the operation of one simulation run.

The model must assess the cumulative impact of this stray current on the rails, the stray current collection system, and any surrounding metallic infrastructure.

As an example of the approach taken to convert the values of current from the model to lifetime, ten interconnected 8-mm bars are used to form the stray current mat placed under the rail. When the current leaks onto the mat (from the rail) and off the mat (into the soil), it is assumed that the current will be evenly distributed over the whole mat but only on half of the bar closest to the interface. This assumption is based on studies of an entire mat within the CDEGS software [1], [8].

Therefore, for 1 m of stray current control mat, the surface area vulnerable to corrosion is

$$0.5 \times \pi \times 10 \times 8 \text{ mm} \times 1000 \text{ mm} = 125\,664 \text{ mm}^2.$$

The current flowing onto/leaving the mat at a particular location can be converted to a current density using this area, and the corrosion rate (for areas where the current is leaving the mat) can be determined using

$$Corrosion\_rate = \frac{Icorr}{nF} \tag{1}$$

where $Icorr$ is the corrosion current density in amperes per square meter, $F$ is Faraday's constant (96 490 C/mole), and $n$ is the number of electrons transferred per molecule of a metal corroded. The corrosion rate is the number of corroded moles of metal per square meter per second, which converts to grams per square meter per day by multiplying with the atomic weight of the metal.

Figs. 16 and 17 show an example of the application of the model and this equation. These graphs give the metal loss that will be observed along the entire length of track bed bars and on the entire length of metallic pipe in one year for the vertical four-layer soil structure.

For the oxygenated areas of the system, the depth of steel corrosion required to cause cracking of the concrete and thus allow rapid penetration of the chloride ions to the steel is typically thought to be in the range of 150–200 $\mu$m. Using this thickness to estimate the life of the system, Figs. 16 and 17 also illustrate the corrosion life calculation of a section of a track bed and of the metallic pipe based on the 150-$\mu$m threshold for the vertical four-layer soil structure.

Significant peaks of corrosion, which correspond to points with lower lifetimes, can be seen in the system as a result of the soil interfaces. The relatively large rail resistance to earth utilized in this paper—consequently low value of current leakage (as obtained from a new system under construction)—is the main reason why the lifetimes of the design structures are high.

The results seen are not simple to interpret and show the need for the use of a software tool in this form of lifetime prediction. In areas of the system with a lower lifetime, an extra stray current management in the form of an upgraded rail insulation, larger track bed conductors, or a stray current control cable could be used to give a longer system lifetime.

This is the main benefit of this form of modeling approach, i.e., the ability to define an economic stray current control system. Care should be taken, however, from corrosion specialists at the postprocessing stage of the stray current analysis. It is necessary to account for electrochemical electromotive forces that will accelerate the corrosion rate and, therefore, diminish the lifetime of the buried structures.

## VI. Conclusion

A simulation model that employs a resistive network to solve the stray current distribution found in/around a dc rail system has been developed. Data for the formulation of the resistive network are provided by CDEGS, which is a commercial tool capable of simulating geometrically accurate systems (such as the track bed mat).

The use of the resistive model significantly reduces the simulation runtime and the central processing unit memory usage when compared with an equivalent CDEGS model. This is not at the expense of accuracy. The very important advantage of the developed model is its ability to be dynamically simulated, in contrast with the CDEGS model, which is realistically restricted to nondynamic case studies within the transit systems.

Furthermore, a four vertical layer soil structure has been modeled (CDEGS is limited to a maximum of three vertical layers). The resistive modeling technique can be utilized to formulate a soil structure with unlimited variations along the route that has no real limitations on length beyond the memory capability of the computer on which it is being run.

This paper uses a resistive model to demonstrate the influence that different soil models have on the corrosion performance of the rail, track bed, and metallic pipe. In a uniform soil environment, severe corrosion on pipelines predominates in sections where there is a low earth resistivity. The horizontally layered soils where the earth resistivity shows a decrease with

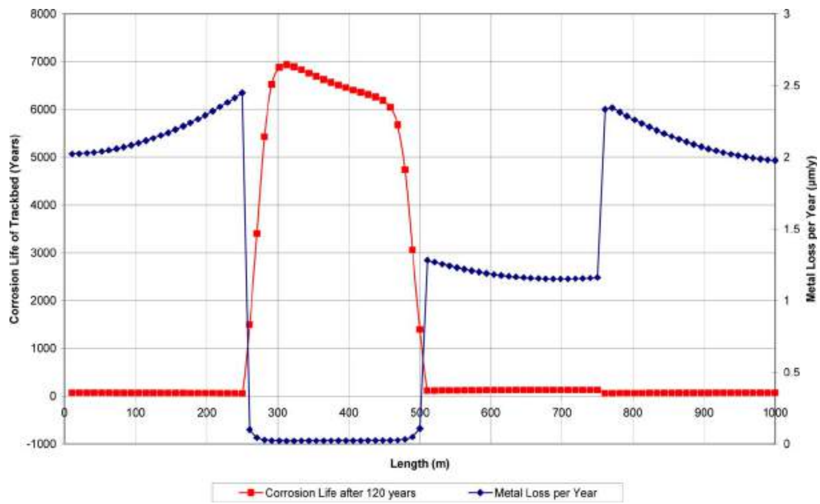


Fig. 16. Metal loss per year and corrosion life of track bed.

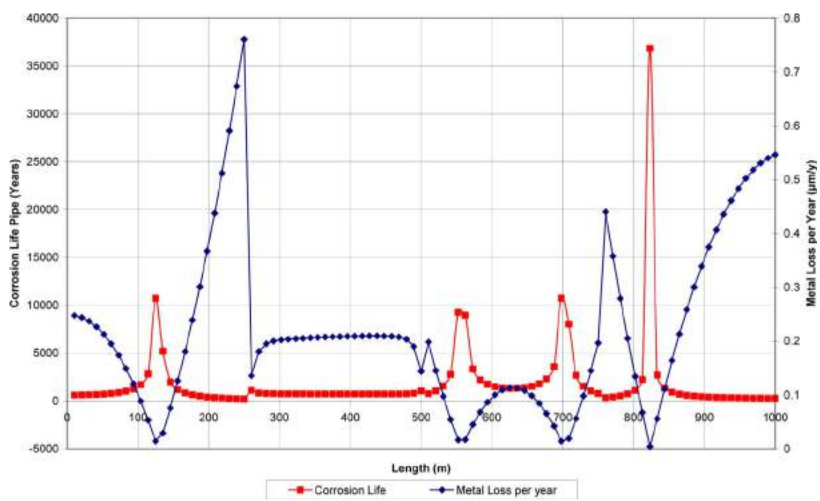


Fig. 17. Metal loss per year and corrosion life of third-party infrastructure.

depth are dominated by the behavior of the upper layer. For vertical models, a concentrated current leakage region will exist on the third-party utility structure and track bed at the point where the soil discontinuity occurs.

The model can be used to optimize the level of stray current protection required along the system length. While this would depend on the provision of accurate soil data, the example used does show how the simulation tool could be used to optimize the stray current control over the length of the system.

## ACKNOWLEDGMENT

The authors would like to thank the valuable technical and financial contribution of CAPCIS Ltd.

## REFERENCES

[1] C. Charalambous and I. Cotton, “Influence of soil structures on corrosion performance of floating DC transit systems,” *Proc. Inst. Electr. Eng.—Elect. Power Appl.*, vol. 1, no. 1, pp. 9–16, Jan. 2007.

[2] C. Charalambous and I. Cotton, “Impact of soil topologies on stray current performance of a DC mass transit system,” in *Proc. XIVth Int. Symp. High Voltage Eng.*, Beijing, China, Aug. 25–29, 2005.

[3] I. Cotton, C. Charalambous, P. Ernst, and P. Aylott, “Stray current control in DC mass transit systems,” *IEEE Trans. Veh. Technol.*, vol. 54, no. 2, pp. 722–730, Mar. 2005.

[4] J. G. Yu, “The effects of earthing strategies on rail potential and stray currents in DC transit railways,” in *Proc. Int. Conf. Develop. Mass Transit Syst.*, Apr. 20–23, 1998, pp. 303–309.

[5] S. Case, “So what’s the problem?” in *Proc. IEE Semin. DC Traction Stray Current Control—Offer Stray Good Ohm?* Oct. 21, 1999, pp. 1/1–1/6. (Ref. 1999/212).

[6] J. G. Yu, “The effects of earthing strategies on rail potential and stray currents in DC railways,” in *Proc. IEE Int. Conf. Develop. Mass Transit Syst.*, London, U.K., 1998, pp. 303–309.

[7] *CDEGS Software*, Safe Eng. Services Technol. Ltd., Montréal, QC, Canada, 1978.

[8] C. Charalambous, “Stray current control and corrosion limitation for DC mass transit systems,” Ph.D. dissertation, Univ. Manchester, Manchester, U.K., Sep. 2005.

[9] J. Ma and F. P. Dawalibi, “Study of influence of buried metallic structures on soil resistivity measurements,” *IEEE Trans. Power Del.*, vol. 13, no. 2, pp. 356–365, Apr. 1998.

[10] T. Takahashi and T. Kawase, “Calculation of earth resistance for a deep-driven rod in a multi-layer earth structure,” *IEEE Trans. Power Del.*, vol. 6, no. 2, pp. 608–614, Apr. 1991.

[11] K. S. Bahra and R. B. Catlow, “Control of stray currents for DC traction systems,” in *Proc. Int. Conf. Elect. Railways United Eur.*, Mar. 27–30, 1995, pp. 136–142.

[12] *Code of Practice for Earthing,* BS 7430, 1998.

**Charalambos A. Charalambous** (M'05) was born in Nicosia, Cyprus, in 1979. He received the Class I B.Eng. degree (Hons.) in electrical and electronic engineering and the Ph.D. degree in electrical power engineering from The University of Manchester, Manchester, U.K., in 2002 and 2005, respectively.

He is currently a Research Associate with the National Grid High Voltage Research Center, University of Manchester. His current research interests include low-frequency transformer modeling, transient studies, and the electrical control and analysis of dc corrosion.

**Ian Cotton** (M'98–SM'07) was born in the U.K. in 1974. He received the Class I B.Eng. degree (Hons.) in electrical engineering from the University of Sheffield, Sheffield, U.K., in 1995 and the Ph.D. degree in electrical engineering from The University of Manchester, Manchester, U.K., in 1998.

He is currently a Lecturer with the Electrical Energy and Power Systems Group, School of Electrical and Electronic Engineering, University of Manchester. His current research interests include power systems transients, the use of higher voltage systems in aerospace applications, and power-system-induced corrosion.

Dr. Cotton is a member of the Institution of Electrical Engineers and a Chartered Engineer.

**Pete Aylott** was born in London, U.K., in 1959. He received the M.A. degree (Hons.) in natural sciences from the University of Cambridge, Cambridge, U.K., in 1981.

Since 1985, he has been with CAPCIS Ltd., Manchester, U.K., where he is currently the Director for Infrastructure Projects. His consultancy experience covers the management of stray current on light rail and heavy rail underground systems and the interactions between these and the utility systems both across the U.K. and overseas.

# A Simulation Tool to Predict the Impact of Soil Topologies on Coupling Between a Light Rail System and Buried Third-Party Infrastructure

Charalambos A. Charalambous, *Member, IEEE*, Ian Cotton, *Senior Member, IEEE*, and Pete Aylott

***Abstract*—The production of stray currents by dc light rail systems leads to the corrosion of the supporting and third-party infrastructure in close proximity to the rail system. This paper simulates two parallel tracks that are occupied by two trains: one on each track. This type of modeling constitutes a case study that is utilized to investigate the effect of soil topologies on the corrosion performance of a floating dc light rail system focusing on the supporting and third-party infrastructure. The modeling technique used involves the accurate computation of the shunt and series parameters for use in a resistive-type model using a commercially available software package. The results demonstrate the importance that soil resistivity has on the corrosion risk to traction system and third-party infrastructure. Such information could ultimately be used to vary the level of stray current protection across a light rail system to ensure a consistent lifetime across the whole system.**

***Index Terms*—Corrosion, dc light rail, soil topologies, stray current.**

## I. Introduction

CURRENT leakage from dc railway systems is an inevitable consequence of the use of the running rails as a mechanical support/guide way and as the return circuit for the traction supply current. Since the rails have a finite longitudinal, or series, resistance (around 40–80 $m\Omega/km$ or 40–80 $\mu\Omega/m$ of rail) and a poor insulation from earth (typically from 2 to 100 $\Omega$km), a proportion of the traction current returning along them will leak to earth and flow along parallel circuits (either directly through the soil or through buried conductors) before returning onto the rail and the negative terminal of the dc rectifier.

Given that the current flow in a metallic conductor is electronic, whereas that through electrolytes such as the earth, concrete, etc., is ionic, it follows that there must be an electron-to-ion transfer as the current leaves the rails to the earth. Where the current leaves the rail to earth, and an anode is produced, there will, therefore, be an oxidation, or electron-producing, reaction.

The corrosion of metallic objects will, therefore, occur from each point that current transfers from a metallic conductor, such as a reinforcement bar in concrete, to the electrolyte (i.e., the concrete). Hence, the stray current leakage can cause corrosion damage to both the rails and any other surrounding metallic elements.

A key factor in determining the level of threat to the third-party infrastructure (utilities) and the supporting infrastructure is the resistivity of the surrounding soil. Typically, a uniform soil resistivity model is assumed over the length of a system. In reality, it will change with both depth and system chainage.

This paper builds on a previous work carried out in [1]–[3]. It describes a simulation tool that can be used to predict the level of stray current (and hence corrosion damage) in a dc light rail system, where the soil resistivity varies in the manner described above. In certain situations where the soil resistivity changes with depth, the buried utilities can experience significant protection from the stray current. However, a sudden change in soil resistivity along the length of the system can concentrate corrosion on a specific location. In such a case, protective measures may be specified at such a location to ensure the system lifetime is not compromised.

The simulation tool accurately calculates the current distribution between the rail, the stray current collection mat, and the buried utility. The modeling technique is demonstrated with a model of two parallel tracks that are occupied by two trains, one on each track. This type of modeling constitutes a realistic case study that can be utilized to investigate the stray current performance of a dc light rail system. Dynamic modeling, as well as static modeling, is possible with this technique. True visualization of the impact of the different soil models on the amount of corrosion seen on the transit system and the surrounding infrastructure is only possible using dynamic models. These dynamic models are essentially time-stepped static models in which the train position and velocity vary as a function of distance.

Since there is a tendency in new transit systems to utilize floating running rails (literature stating that floating running rails are the best option if the stray current is to be minimized [3]–[5]), this paper specifically addresses the corrosion performance of floating dc light rail systems. However, the simulation tool does have the capability to incorporate solidly bonded and diode-bonded systems [6], [8].

Manuscript received September 29, 2006; revised July 27, 2007, September 10, 2007, and September 11, 2007. The review of this paper was coordinated by Mr. D. Diallo.

C. A. Charalambous is with the National Grid High Voltage Research Center, The University of Manchester, M60 1QD Manchester, U.K. (e-mail: charalambos.charalambous@manchester.ac.uk).

I. Cotton is with the School of Electrical and Electronic Engineering, The University of Manchester, M60 1QD Manchester, U.K. (e-mail: ian.cotton@manchester.ac.uk).

P. Aylott is with CAPCIS Ltd., M1 7DP Manchester, U.K.

Color versions of one or more of the figures in this paper are available online at http://ieeexplore.ieee.org.

Digital Object Identifier 10.1109/TVT.2007.909312

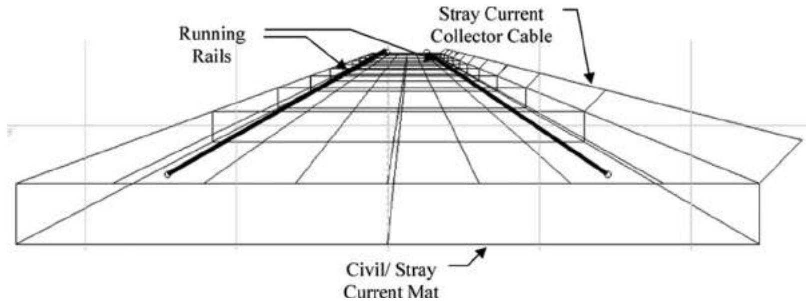


Fig. 1. Geometrically accurate CDEGS model in perspective view.

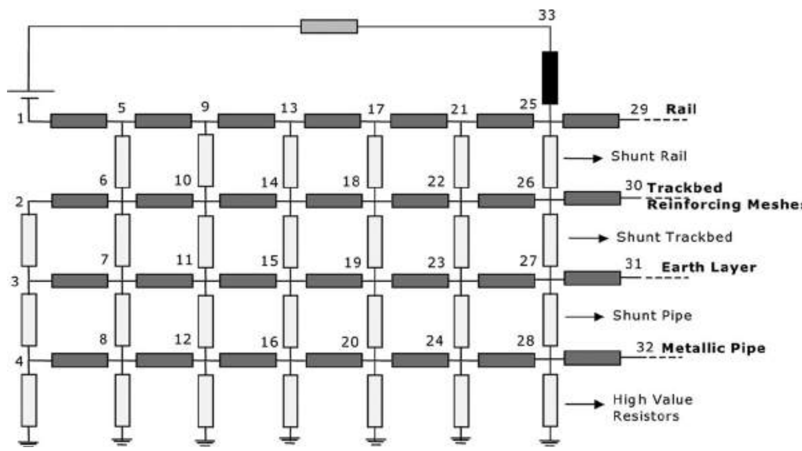


Fig. 2. Resistive network for the rail, track bed, and metallic pipe (floating system).

## II. Model System

### A. Introductory Remarks

The essential elements of a transit system are the rails, the rail-to-earth insulation, the power supply, and the vehicles. The design and placement of these elements of the transit system dictate the stray current performance in terms of the total stray current leaving the rails [1], [3].

The work carried out in [1] described the design principles employed in current distribution, electromagnetic fields, grounding, and soil structure analysis (CDEGS) [7] to accurately model the current distribution between structures of a dc light rail system by taking into consideration the geometry of the system, the soil topology, and the interactions between the metallic structures under study. Fig. 1 illustrates the perspective view of the CDEGS model, for the rails, their supporting infrastructure (track bed), and a third-party infrastructure (e.g., buried metallic pipe).

The work carried out in [2] described a simulation tool that is a two-step process combining the accuracy of CDEGS with the flexibility of a resistive network model implemented in MATLAB. CDEGS is initially used to investigate the self and mutual resistances of metallic structures in various soil structures, taking into consideration factors like buried depth, material of conductor, coating, radius, length, and geometrical arrangement.

The reinforced concrete mat placed underneath the rails is used for both structural support and as a conductive path for the stray current. Connected to this mat is an insulated cable (generally copper) that increases the overall conductivity of the stray current collection circuit relative to the alternative stray current paths in the soil and other buried objects. The CDEGS model effectively calculates a combined resistance parameter for both the track-bed reinforcing bars and the connected collector cable.

The information provided by CDEGS is then appropriately employed in a simplified resistive network that speeds up the simulation time while, at the same time, maintains the accuracy of the results produced. This form of model has a number of advantages, one of them being the fact that it can be dynamically utilized to acquire a true visualization of the stray current corrosion risk. Fig. 2 illustrates the resistive-type network. The components of this model are described in more detail in the next section of this paper.

### B. Description of Static Simulation Model

The described model has been further enhanced to simulate two parallel tracks that are occupied by two trains, one on each track. With this form of modeling, parameters such as the effect of cross bonding the tracks on the stray current level produced by the system can be examined. In dc-electrified railways, it is a common practice for the rails of each track to be bonded together and for the tracks to be cross bonded to reduce the resistance of the return path, thus reducing the generation of stray currents.

As in previous modeling efforts, geometrically accurate models are first built in the software. These models, as shown in Fig. 3, are relatively short in length owing to the high complexity of the model. They are used to develop and validate

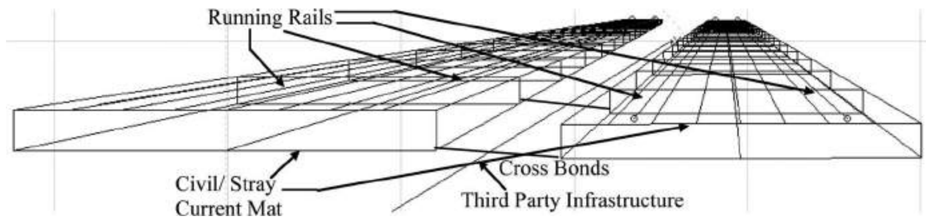


Fig. 3. Geometrically accurate CDEGS model for two tracks in perspective view.

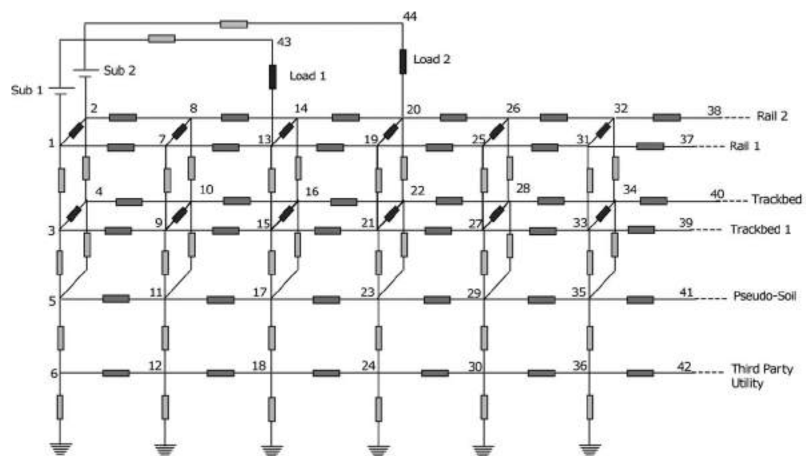


Fig. 4. Resistive-type network for the double-track floating system.

[8] the resistive-type network shown in Fig. 4. If changes in soil resistivity occur over a system length, multiple models would be run to produce different resistive network parameters for each individual case.

The resistive network that has been produced is shown in Fig. 4 and includes (at the top) two sets of resistors that represent the two tracks. For modeling purposes, the equivalent series resistance of each track is represented by one resistor layer based on the assumption that only one rail is used for the return current (the other is used for signaling).

A shunt resistor then represents the resistance of the rail to the track bed (in reality, this is practically the same as the resistance to earth of the rail for most well-coated systems). Below each set of the resistors representing the rails, there also exists a resistor layer that represents the equivalent series and shunt resistance of the track bed (stray current collection mat). Each track has its equivalent track bed situated beneath it.

The third layer is the "pseudo-earth layer," which can be appropriately modified for different soil structures. This layer is important to be included as it is recognized that some current flows through the earth and that this has a finite conductivity. This layer is placed before any third-party infrastructure, as current will always flow from the track bed into the earth before reaching such an infrastructure. The final fourth layer represents the series and shunt resistances of this third-party infrastructure/metallic pipe.

The series resistance of the rail, the metallic mat, and the buried pipe can easily be calculated using the cross-sectional area, length, and resistivity of each conductor's material. The series resistance of the pseudo-earth layer, which varies according to soil resistivity, is determined by an iterative process (the end result requiring the results from a resistive model to match that of the more complex CDEGS model).

Additionally, the resistive model includes four sets of shunt resistors that interconnect the different layers. The role of the shunt resistors in conjunction with the "pseudo-earth layer" is to provide the conductive path between the different structures; these values vary according to the specified soil structure. Of particular note is that the values of shunt resistance for the rail are determined by approximating the resistance of the insulating pads that support the rail on the track bed.

The values of shunt resistance used for the track bed and the metallic pipe are initially determined by CDEGS by determining the resistance to earth of each structure. Simple models (not time consuming) need to run in CDEGS to determine the resistance to earth, according to the specified soil environment.

The resistive model uses the produced database of resistance to earth values (depending on specified soil structures) and can employ those in every consecutive section when multiple soil models are present.

This does not, however, fully reflect the resistance between the individual elements, and the values of these are, therefore, iterated along with the series resistance of the pseudo-earth later to accurately reproduce the CDEGS current distribution in the resistive model.

Of all the parameters detailed in this paper, the value of the soil resistivity used is likely to introduce the greatest source of error into the modeling process. The CDEGS software has been shown to be accurate by many researchers around the world and has been extensively verified.

The models described in this paper are simplifications of a real system (for example, the track bed reinforcement bar would be too complex to allow the modeling of all conductors), but these simplifications were used after confirming that they did not cause an error in any expected current/voltage of more than 1% [1].

The error introduced by the soil resistivity relates to the fact that it is difficult to measure and that it changes as a function of the season/weather conditions. These statements can be qualified by work carried out by other researchers. Ma and Dawalibi state that the soil resistivity measurements can be in error by as much as 50% when measurements are taken in proximity to metallic buried structures [9]. For a new light rail system in an urban environment, it is highly unlikely that such buried structures will not be present.

Other researchers find that soil resistivities can change in a local environment by a factor of 20 according to the level of moisture present within the soil [10]. The soil near the earth boundary is likely to be significantly affected. It would, therefore, be prudent in any analysis to consider likely variations in soil resistivity over a year and the influence of buried objects on measurements before carrying out simulations.

The system that has been studied is modeled on the basis of the parameters given in Table I. Two tracks are modeled along with the track beds that are placed underneath them. The location of cross bonds can be controlled by the user and can be placed every 100 m, 200 m, 300 m, etc. In this case, the tracks are cross bonded every 100 m, as is the track bed itself. Cross bonds have been shown to be beneficial in controlling the levels of stray current on a floating dc light rail system [11].

It is noted that the model has the capability of modeling randomly spaced cross bonds. It is also possible not to include cross bonds (isolating the tracks by using high value resistors) or to randomly select which cross bonds are conducting. Consequently, the cases where the train locations do not coincide with the cross-bond locations can be investigated.

TABLE I
DESIGN PARAMETERS OF THE SIMULATION MODEL

| | | |
|---|---|---|
| RAILS | Series Resistance: | 0.04 Ω/km |
| | Resistance to earth: | 320 Ωkm |
| | Number of conductors: | 1 |
| | Buried at depth: | 0.05 m |
| METALLIC MATS | Series Resistance: | 0.08 Ω/km |
| | Resistivity of Coating: | 180 Ωm / thickness 40 mm |
| | Radius: | 0.0094 m |
| | Number of conductors: | 10 longitudinal |
| | Buried at depth: | 0.628 m |
| PIPES | Series Resistance: | 1.437 mΩ/km |
| | Radius: | Ext: 0.61 m Int: 0.512 m |
| | Number of conductors: | 1 hollow |
| | Buried at depth: | 20.628 m |
| CROSS BONDS | Series Resistance: | 1.437 mΩ |
| | Cross Sectional Area: | 120 $mm^2$ |
| | Number of conductors: | Every 100 m |
| | Length: | 10 m |
| POWER | Train current: | 1000 A |

## C. *Validation of Static Simulation Model*

As a starting point, the system is modeled in CDEGS. The capability of the software to select shunt and series parameters is utilized with the ultimate purpose of establishing an agreement between CDEGS and resistive network results in terms of the stray current distribution between the different metallic structures.

The models shown in Figs. 3 and 4 are implemented in MATLAB using the resistive model. Equivalent geometrically accurate systems were also developed in CDEGS. All of the models used in this section relate to systems placed in a soil resistivity of 100 Ωm. Validations of the shunt/series parameters used later in this paper for the alternative soil models have been carried out but are not presented.

The first case study (i.e., Fig. 5) illustrates a 1-km section of two parallel tracks, which represent the geometrically accurate CDEGS model of Fig. 3. These 1-km sections are representative of a symmetrical 2-km section of two parallel tracks with two trains at the center of each track and a substation at the same end of each track, drawing a constant current of 1000 A each.

This static model assumes worst-load conditions; it thus constitutes a worst-case scenario for modeling the impact of stray current on the rails, the track bed, and the third-party utility structure. It is, however, noted that for a double-end feeding situation, more trains in the section will result in more current demands and, hence, greater leakage current. The so-called worst-case scenario, when considering a single train fed from one substation, is just a quick preliminary crude assessment for the stray current performance, and this is how it is perceived by the authors.

Figs. 6 and 7 illustrate a comparison of the results obtained by CDEGS simulations using the static models presented in Fig. 3 and by simulation of the resistive-type network (Fig. 5) in the case where the tracks are cross bonded. The graphs show the net current leakage profiles of the stray current collection mat (track bed) and the third-party utility.

The net current leakage is taken to be the difference between the stray current entering the structure and that leaving the structure (for example, on a track bed, the current may enter at the top of the track bed, some will then exit at the base, and the remainder being carried along the track bed). The maximum difference between the results from the MATLAB resistive model and those obtained by CDEGS is 2.2%.

The results are those expected when a floating rail system is simulated, i.e., one half of the system shows current flowing into the metallic conductors, whereas the other half of the system shows current leaving the conductors.

The second case study in Fig. 8 considers the same basic model used in case study I but has the position of the load

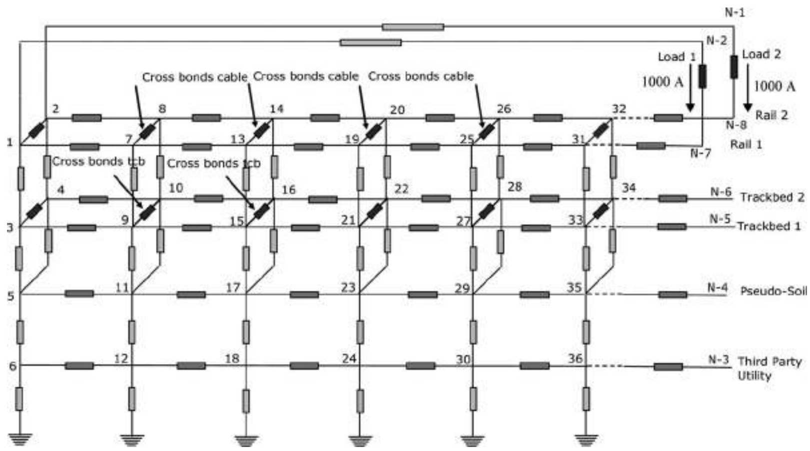


Fig. 5. Resistive-type network, substations same end (case study I).

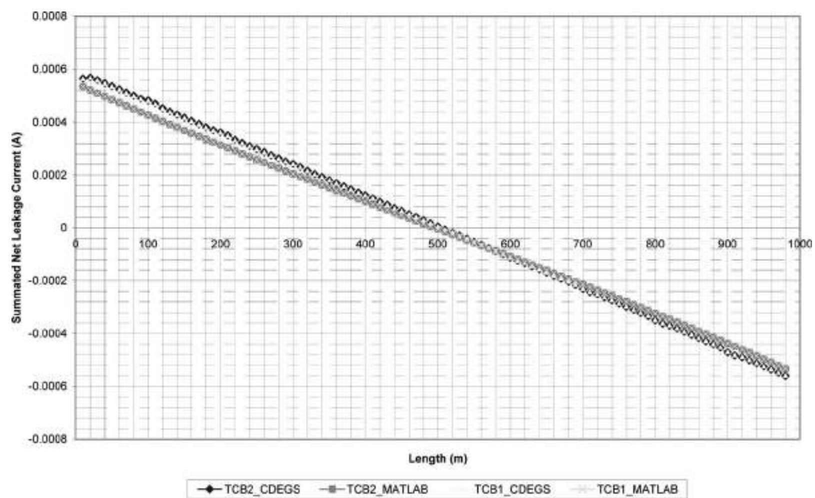


Fig. 6. Summated net current leakage of track beds obtained by CDEGS and MATLAB with the tracks cross bonded (case study I).

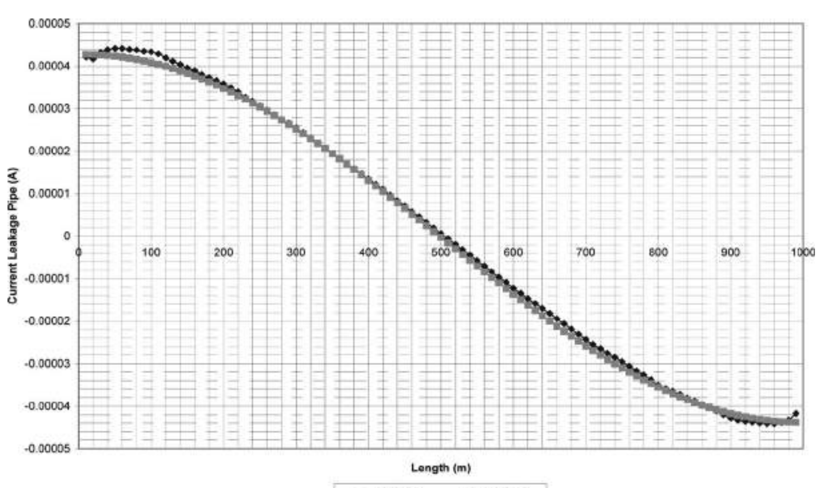


Fig. 7. Summated net current leakage of the third-party utility obtained by CDEGS and MATLAB with the tracks cross bonded (case study I).

(train) and the substation swapped on one of the tracks. The objective of this case study is to demonstrate the effect of substation placement on the stray current level of the rails and the third-party infrastructures in addition to the effect of cross bonding the two tracks. The values of the shunt parameters in the resistive network of Fig. 8 have not been altered and are the same as those employed in the case study in Fig. 5.

Figs. 9 and 10 illustrate a comparison of the results obtained by CDEGS simulations using the models presented in Fig. 3 (the direction of currents is reversed to cope with the change

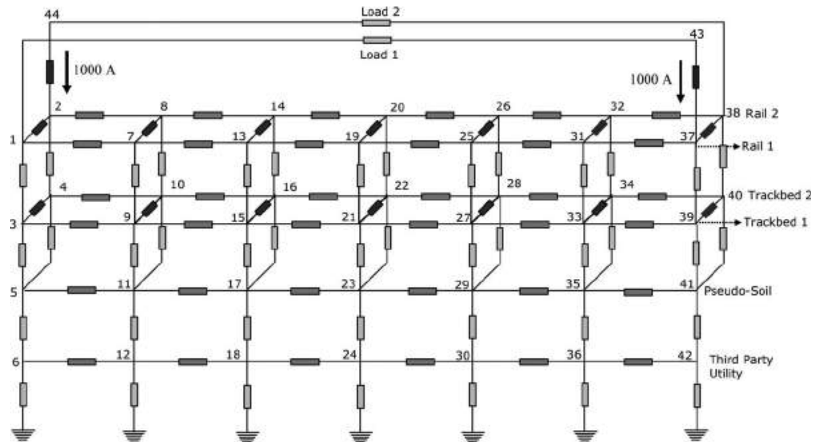


Fig. 8. Resistive-type network, substations opposite end (case study II).

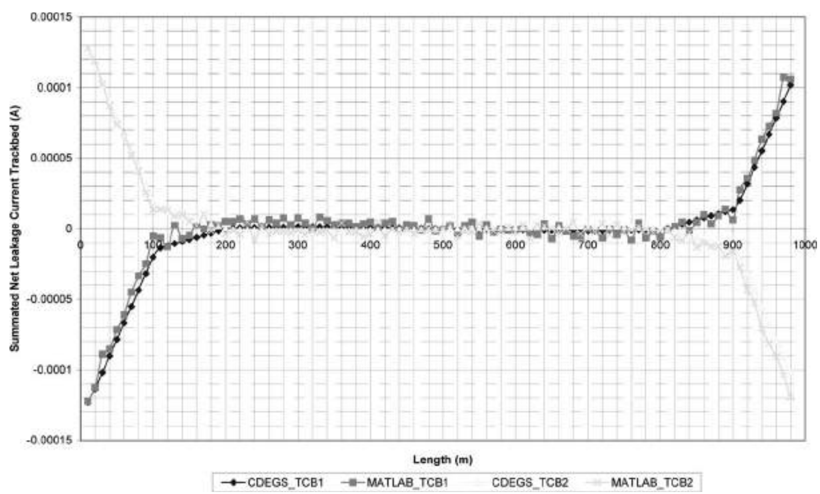


Fig. 9. Summated net current leakage of track beds obtained by CDEGS and MATLAB with the tracks cross bonded (case study II).

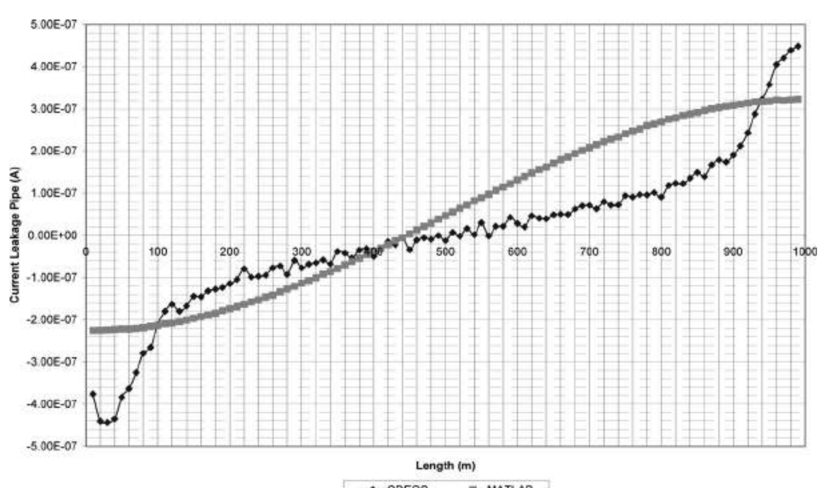


Fig. 10. Summated net current leakage of the third-party utility obtained by CDEGS and MATLAB with the tracks cross bonded (case study II).

of substation placement) and by simulation of the resistive-type network (Fig. 8).

The results presented in Fig. 9 show a good agreement between the MATLAB and CDEGS models, although the level of stray current is significantly less (a maximum value of just under 0.15 mA is observed, in comparison to 0.6 mA in the previous case). The reduction in the level of stray current relates to the flow of traction current in opposite directions and the ultimate cancellation due to the cross bonds connecting the two tracks. The stray current will not be reduced to zero, owing to the finite resistance of the track between the cross-bond locations and the resistance of the cross bonds themselves.

In the first case, a maximum current slightly lower than 0.5 $\mu$A is seen entering the pipe. In the second case, the simulations show an increased error between the MATLAB and CDEGS computations. However, in this case, the maximum current seen entering the pipe is less than 0.5 $\mu$A, according to CDEGS and just over 0.2 $\mu$A according to MATLAB. The discrepancy is attributed to the numerical error introduced into the CDEGS results by a matrix inversion process. The error introduced becomes significant at this level of current. However, this level of current is so small that it is not of concern when it is to be used to consider corrosion risk.

The fact that identical series and shunt resistance parameters (for the rails, the track beds, the earth layer, and the third-party utility structure) were employed in both resistive-type network models (Figs. 5 and 8) and that the results obtained from the developed algorithm in MATLAB and CDEGS modeling are consistent gives confidence in the validity of the proposed simulation tool.

The runtime simulation of the developed algorithm in MATLAB is dramatically reduced when compared with the runtime simulation that an equivalent model in CDEGS requires. This directly relates to the number of elements required to accurately simulate the system and, therefore, to the maximum system size that could be simulated as well (this being driven by memory capacity).

This reduction in the simulation runtime and enhancement of the system size that could be studied does not come at the expense of the accuracy of the results.

Table II tabulates the percentage of discrepancy in the current leakage profiles of the elements employed in this paper. The presented data are weighted averages of the discrepancies (CDEGS versus MATLAB values) of the current leakage along the entire length of each structure (total stray current). Additionally, the table provides a comparison of the computation time monitored for each model. The physical description of the models is given in Table III.

### D. *Investigation of the Effect of Alternative Soil Structures*

The purpose of this paper is to examine the impact of different soil structures on the stray current distribution. CDEGS allows the user to define the characteristics of the soil in which the conductors are being modeled. If the soil is not uniform, a layered soil model can be specified.

A maximum of three horizontal earth layers or three vertical earth layers may be specified in terms of their resistivity and layer thickness. CDEGS could, therefore, allow the construction of resistive models of systems placed in different soil environments. In terms of implementing this into the resistive model, a system that is considered to pass through three different soil resistivity regions would require three sets of shunt/series parameters from three different CDEGS simulations, all using the alternative soil resistivity values.

In this paper, simulations using uniform soils, two-layer horizontal soils, and two-layer vertical soil resistivity environments are presented, utilizing the resistive model simulation tool developed. Ultimately, the simulation tool can be utilized to formulate a soil structure with unlimited variations along the route [8]. Table III gives the specific details of the various models used in this paper.

The uniform soil models employed in this paper are representative of the soil structures, e.g., 10 $\Omega$m corresponds to wet organic soil, 100 $\Omega$m corresponds to moist soil, and 1000 $\Omega$m corresponds to dry soil [12].

Uniform models A and B allow all of the systems to be enclosed by the same soil resistivity (although the rails remain coated by a high-resistivity layer to enable simulation of the correct rail-to-earth resistance and the track bed conductors are coated with a layer equivalent in thickness and resistivity to the cover provided by the track bed concrete).

In the case of the two-layer horizontal models, the rail and the track bed both lie in the top layer, whereas the metallic pipe lies in the bottom layer. The track bed and rail are placed into the same environment, as they are in close proximity to real dc light rail systems. The two simulated models represent the cases where the soil resistivity increases with depth (model C) and the case where the resistivity decreases with depth (model D).

For the two-layer vertical models, the rail, metallic mat, and pipe all see a change in soil resistivity at a distance of 500 m, i.e., half of their length lies in a high-resistivity soil, whereas the other half lies in a low-resistivity soil.

For the four-layer vertical models, the rail, metallic mat, and pipe all see a change in soil resistivity at a distance of 250 m, i.e., a quarter of their length lies in a 10-$\Omega$m resistivity soil, a quarter of their length lies in a 100-$\Omega$m resistivity soil, a quarter of their length lies in a 1000-$\Omega$m resistivity soil, and the last quarter lies in a 10-$\Omega$m resistivity soil.

## III. Dynamic Modeling

In this section, a simple dynamic model has been used in which a train is moved along a 1000-m section of track while drawing a constant current (to represent running at constant velocity on a constant gradient). The stray current assessment has been based on an equivalent effective traction current of 1000 A. The results may be scaled to other traction currents if desired, as this is a linear system.

By monitoring the total positive stray current (i.e., current leaking off a metallic structure) during each time step of the simulation, the total corrosive stray current can be obtained by its integration. This is defined as the gross leakage charge. The negative stray current, i.e., that returning onto structures, is not considered as this does not cause any corrosion to take place and does not reverse the corrosion process caused by a positive stray current leakage.

The simulation results presented in Section IV are based on a scenario in which two substations are placed at opposite ends of two tracks and in which the trains are moved in opposite directions, as illustrated in Fig. 11. The two tracks are cross bonded.

There is no particular significance in the choice of the system, and the results that have been obtained will, therefore, only serve to give conclusions that relate to the importance of the accurate simulation of soil structures.

TABLE II
PERCENTAGE OF DISCREPANCY TOTAL STRAY CURRENT ON METALLIC STRUCTURES: A COMPARISON BETWEEN CDEGS AND MATLAB

| | % Discrepancy in results CDEGS – MATLAB model | | | Computation Time (seconds) | |
|---|---|---|---|---|---|
| **Soil Structures** | **Rail** | **Trackbed** | **Metallic Pipe** | **CDEGS** | **MATLAB** |
| **Model A-Uniform** | 0.13 % | 1.69% | 2.08 % | 91.50 | 3.3 |
| **Model B-Uniform** | 0.36 % | 0.92% | 0.18% | 91.53 | 3.3 |
| **Model C-Horizontal** | 0.14% | 2% | 7.6% | 127.1 | 4 |
| **Model D- Horizontal** | 0.35% | 0.95% | 0.0318% | 205.35 | 4 |
| **Model E- Vertical** | 0.23% | 3.87% | 0.9% | 326.7 | 5 |

TABLE III
MODELS EMPLOYED IN SIMULATIONS

| | | |
|---|---|---|
| **UNIFORM MODEL** | | |
| Model A | 10 Ω.m | 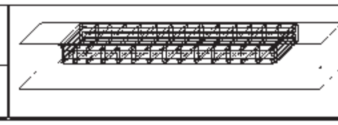 |
| Model B | 1000 Ω.m | |
| **TWO LAYER HORIZONTAL MODEL** | | |
| Model C | *Top Layer*:10 Ω.m /*Bottom Layer*:1000 Ω.m | 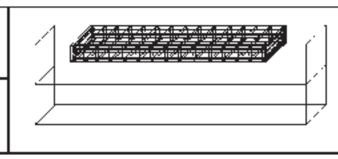 |
| Model D | *Top Layer*:1000Ω.m /*Bottom Layer*:10Ω.m | |
| **TWO LAYER VERTICAL MODEL** | | |
| Model E | *Front Layer*:10 Ω.m / *Back Layer*:1000 Ω.m | 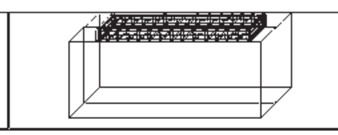 |
| **FOUR LAYER VERTICAL MODEL** | | |
| Model F | *A Layer*:10 Ω.m / *B Layer*:100 Ω.m/ *C Layer*:1000 Ω.m/ *D Layer*:10 Ω.m | 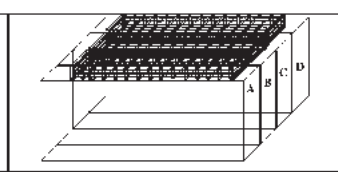  |

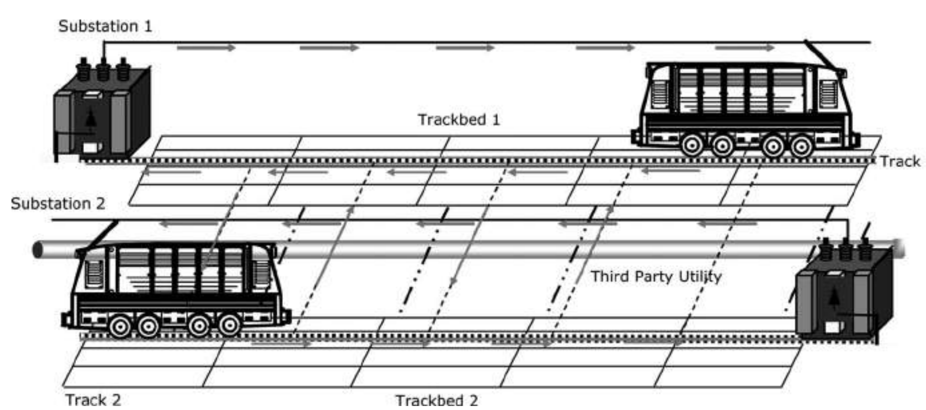


Fig. 11. Schematic arrangement of simulation model (substations opposite end).

Fig. 12 illustrates a flowchart of the operation of the software in terms of the calculation of the stray current distribution for each static model and the procedure that then determines the gross leakage charge of the rails, track beds, and third-party utility structure.

## IV. SIMULATION RESULTS

When the system is simulated with one movement of the trains, i.e., from one end of the track to the other (respectively), the gross leakage charge for all of the individual system elements can be described. The gross leakage charge of the rail

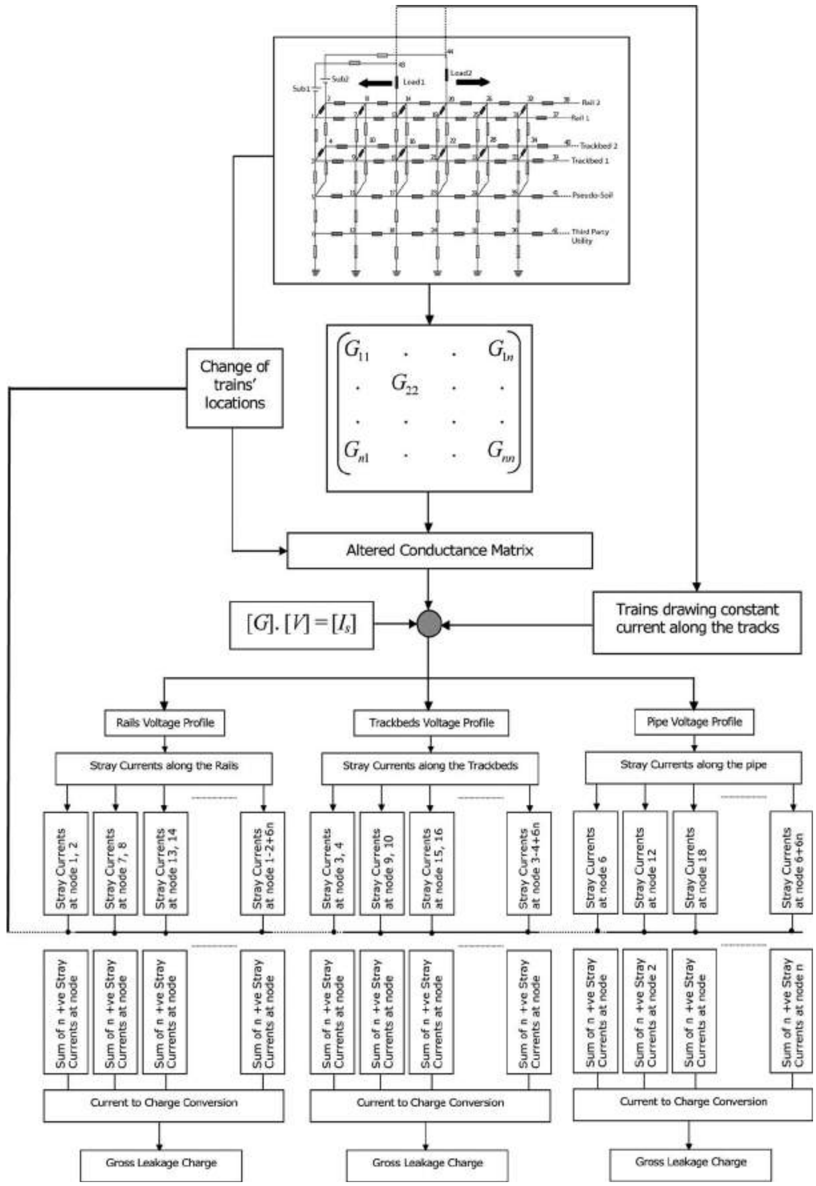


Fig. 12. Flow chart to determine the gross leakage charge.

is the same for all the soil resistivity models due to the high resistance of the coating layer placed along the rails. Fig. 13 illustrates the cumulative leakage charge profile for all three uniform model cases.

Fig. 14 illustrates the corrosive leakage charge of the base of the track bed for all soil resistivity models except F (this is used later in the paper). Only the base of the track bed is considered since the corrosion at the top of the track bed is assumed to be proportional to the rail leakage current (owing to the direction in which the current will flow into the track bed from the rails) and is, therefore, invariant as a function of soil resistivity.

Fig. 14 shows the significant impact of the vertical soil structure (model E) on the leakage current with a large discontinuity being present at the soil structure boundary. It is significant that in the lowest soil resistivity region (10 Ωm at 0–500 m), the observed leakage currents are higher than those seen in soil model A, which has a uniform resistivity of 10 Ωm.

When comparing models B and D, the performance of the track bed stays reasonably constant, although in D, the bottom layer resistivity has significantly decreased from 1000 to 10 Ωm. The reason for the performance of the track bed staying reasonably constant is the high reflectivity factor at the boundary between the top and bottom soil layers. When the upper layer resistivity is large in comparison to the lower layer (as in model D), the reflection index is approximately 1, and the current cannot penetrate into the lower layer [9]. The current can, therefore, not easily reach the pipe or the lower resistivity and is retained on the track bed in a similar way as the 1000-Ωm uniform soil model.

When comparing models A and C, the bottom layer resistivity increases from 10 to 1000 Ωm, and the level of gross leakage charge on the base of the track bed is seen to significantly decrease [1].

Fig. 15 illustrates the cumulative corrosive leakage charge of the third-party utility structure (metallic pipe) for all the soil resistivity models (except F) tabulated in Table II.

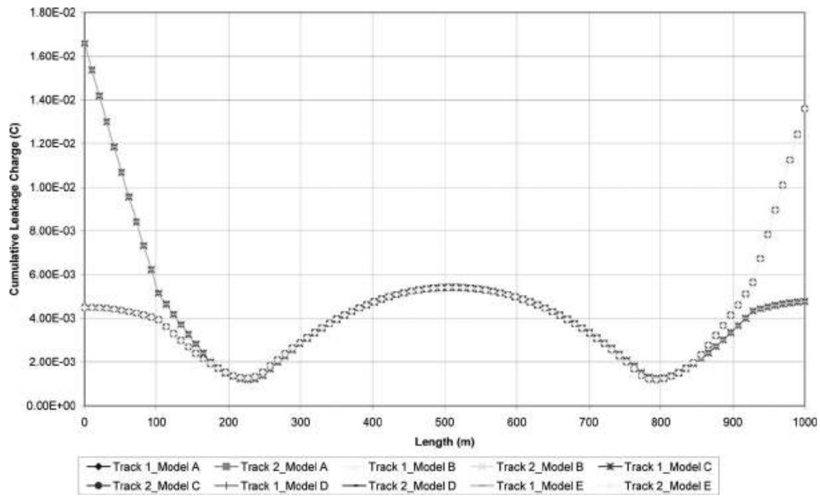


Fig. 13. Cumulative leakage charge rails.

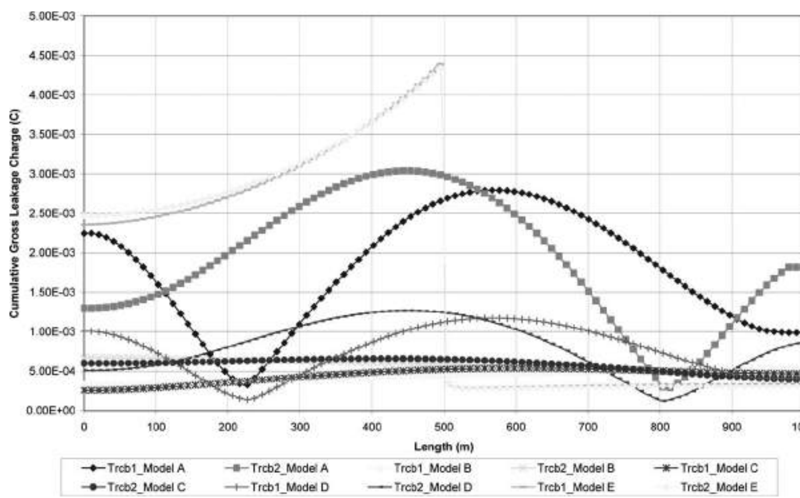


Fig. 14. Cumulative leakage charge base of the track beds.

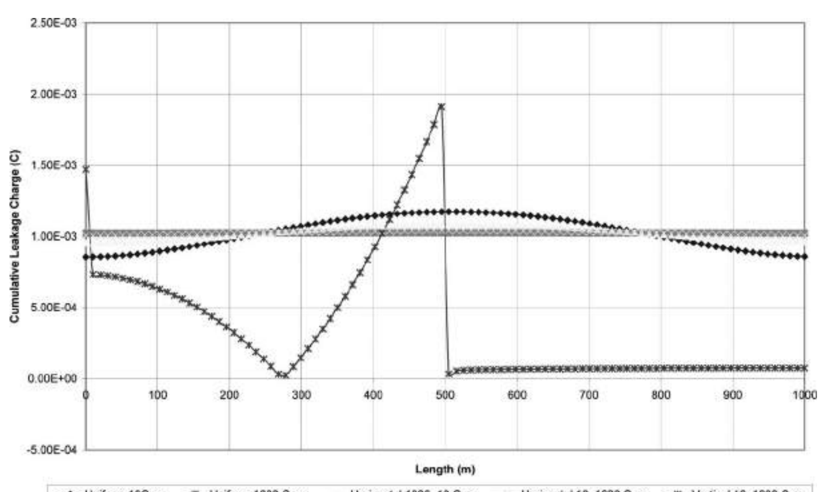


Fig. 15. Cumulative leakage charge of the third-party infrastructure.

The results for the vertical soil model E verify the previous conclusions [1], i.e., that a concentrated current leakage region will exist on the third-party utility structure and track bed when a vertical soil model exists. The discontinuities highlighted in Figs. 14 and 15 show that some portions of the system around the soil interfaces are more at risk.

The results shown in Fig. 15 also illustrate the fact that in homogenous systems, high soil resistivities mean that the third-party buried structures are less vulnerable to corrosion damage, whereas in low soil resistivities, the converse is true.

## V. Example of Modeling a Real System

This paper is intended to aid in the accurate modeling of real transit systems. This example of modeling utilizes Model F, which is a four-layer vertical soil structure, as illustrated in Table II. The details on the technique utilized to formulate a multilayer soil structure are given in [8]. An example of the use of modeling in the analysis of a simple system is now presented.

The model consists of two 1-km tracks, as shown in Fig. 11, on which the trains move with a constant velocity in opposite directions and, hence, draw a constant current. The current used in this simulation is 1000 A. The results could be linearly scaled for other values of current.

The operational condition is that the trains move along the section of track with a headway of 3 min. This will result in 20 trains running per hour on each track (therefore, 40 trains per hour on both tracks). Assuming that services are running for 19 h, i.e., from 5 A.M. until midnight, the total number of trains that will run across the section of two tracks under study would be 760. Therefore, the total charge produced by the movement of 760 trains will be 760 times more than the charge produced by the operation of one simulation run.

The model must assess the cumulative impact of this stray current on the rails, the stray current collection system, and any surrounding metallic infrastructure.

As an example of the approach taken to convert the values of current from the model to lifetime, ten interconnected 8-mm bars are used to form the stray current mat placed under the rail. When the current leaks onto the mat (from the rail) and off the mat (into the soil), it is assumed that the current will be evenly distributed over the whole mat but only on half of the bar closest to the interface. This assumption is based on studies of an entire mat within the CDEGS software [1], [8].

Therefore, for 1 m of stray current control mat, the surface area vulnerable to corrosion is

$$0.5 \times \pi \times 10 \times 8 \text{ mm} \times 1000 \text{ mm} = 125\,664 \text{ mm}^2.$$

The current flowing onto/leaving the mat at a particular location can be converted to a current density using this area, and the corrosion rate (for areas where the current is leaving the mat) can be determined using

$$Corrosion\_rate = \frac{Icorr}{nF} \quad (1)$$

where $Icorr$ is the corrosion current density in amperes per square meter, $F$ is Faraday's constant (96 490 C/mole), and $n$ is the number of electrons transferred per molecule of a metal corroded. The corrosion rate is the number of corroded moles of metal per square meter per second, which converts to grams per square meter per day by multiplying with the atomic weight of the metal.

Figs. 16 and 17 show an example of the application of the model and this equation. These graphs give the metal loss that will be observed along the entire length of track bed bars and on the entire length of metallic pipe in one year for the vertical four-layer soil structure.

For the oxygenated areas of the system, the depth of steel corrosion required to cause cracking of the concrete and thus allow rapid penetration of the chloride ions to the steel is typically thought to be in the range of 150–200 $\mu$m. Using this thickness to estimate the life of the system, Figs. 16 and 17 also illustrate the corrosion life calculation of a section of a track bed and of the metallic pipe based on the 150-$\mu$m threshold for the vertical four-layer soil structure.

Significant peaks of corrosion, which correspond to points with lower lifetimes, can be seen in the system as a result of the soil interfaces. The relatively large rail resistance to earth utilized in this paper—consequently low value of current leakage (as obtained from a new system under construction)—is the main reason why the lifetimes of the design structures are high.

The results seen are not simple to interpret and show the need for the use of a software tool in this form of lifetime prediction. In areas of the system with a lower lifetime, an extra stray current management in the form of an upgraded rail insulation, larger track bed conductors, or a stray current control cable could be used to give a longer system lifetime.

This is the main benefit of this form of modeling approach, i.e., the ability to define an economic stray current control system. Care should be taken, however, from corrosion specialists at the postprocessing stage of the stray current analysis. It is necessary to account for electrochemical electromotive forces that will accelerate the corrosion rate and, therefore, diminish the lifetime of the buried structures.

## VI. Conclusion

A simulation model that employs a resistive network to solve the stray current distribution found in/around a dc rail system has been developed. Data for the formulation of the resistive network are provided by CDEGS, which is a commercial tool capable of simulating geometrically accurate systems (such as the track bed mat).

The use of the resistive model significantly reduces the simulation runtime and the central processing unit memory usage when compared with an equivalent CDEGS model. This is not at the expense of accuracy. The very important advantage of the developed model is its ability to be dynamically simulated, in contrast with the CDEGS model, which is realistically restricted to nondynamic case studies within the transit systems.

Furthermore, a four vertical layer soil structure has been modeled (CDEGS is limited to a maximum of three vertical layers). The resistive modeling technique can be utilized to formulate a soil structure with unlimited variations along the route that has no real limitations on length beyond the memory capability of the computer on which it is being run.

This paper uses a resistive model to demonstrate the influence that different soil models have on the corrosion performance of the rail, track bed, and metallic pipe. In a uniform soil environment, severe corrosion on pipelines predominates in sections where there is a low earth resistivity. The horizontally layered soils where the earth resistivity shows a decrease with

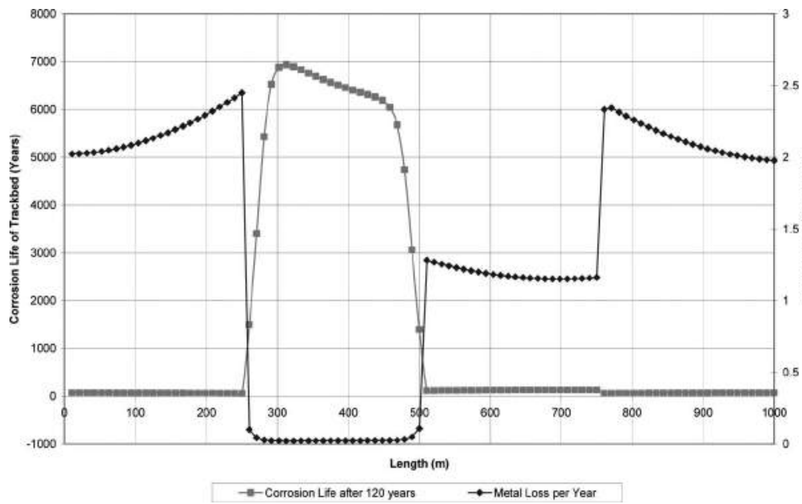


Fig. 16. Metal loss per year and corrosion life of track bed.

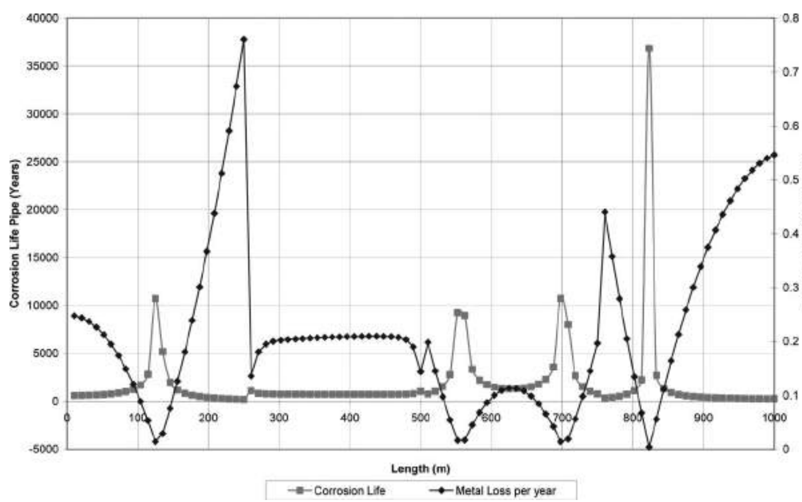


Fig. 17. Metal loss per year and corrosion life of third-party infrastructure.

depth are dominated by the behavior of the upper layer. For vertical models, a concentrated current leakage region will exist on the third-party utility structure and track bed at the point where the soil discontinuity occurs.

The model can be used to optimize the level of stray current protection required along the system length. While this would depend on the provision of accurate soil data, the example used does show how the simulation tool could be used to optimize the stray current control over the length of the system.

## ACKNOWLEDGMENT

The authors would like to thank the valuable technical and financial contribution of CAPCIS Ltd.

## REFERENCES

[1] C. Charalambous and I. Cotton, "Influence of soil structures on corrosion performance of floating DC transit systems," *Proc. Inst. Electr. Eng.—Elect. Power Appl.*, vol. 1, no. 1, pp. 9–16, Jan. 2007.

[2] C. Charalambous and I. Cotton, "Impact of soil topologies on stray current performance of a DC mass transit system," in *Proc. XIVth Int. Symp. High Voltage Eng.*, Beijing, China, Aug. 25–29, 2005.

[3] I. Cotton, C. Charalambous, P. Ernst, and P. Aylott, "Stray current control in DC mass transit systems," *IEEE Trans. Veh. Technol.*, vol. 54, no. 2, pp. 722–730, Mar. 2005.

[4] J. G. Yu, "The effects of earthing strategies on rail potential and stray currents in DC transit railways," in *Proc. Int. Conf. Develop. Mass Transit Syst.*, Apr. 20–23, 1998, pp. 303–309.

[5] S. Case, "So what's the problem?" in *Proc. IEE Semin. DC Traction Stray Current Control—Offer Stray Good Ohm?* Oct. 21, 1999, pp. 1/1–1/6. (Ref. 1999/212).

[6] J. G. Yu, "The effects of earthing strategies on rail potential and stray currents in DC railways," in *Proc. IEE Int. Conf. Develop. Mass Transit Syst.*, London, U.K., 1998, pp. 303–309.

[7] *CDEGS Software*, Safe Eng. Services Technol. Ltd., Montréal, QC, Canada, 1978.

[8] C. Charalambous, "Stray current control and corrosion limitation for DC mass transit systems," Ph.D. dissertation, Univ. Manchester, Manchester, U.K., Sep. 2005.

[9] J. Ma and F. P. Dawalibi, "Study of influence of buried metallic structures on soil resistivity measurements," *IEEE Trans. Power Del.*, vol. 13, no. 2, pp. 356–365, Apr. 1998.

[10] T. Takahashi and T. Kawase, "Calculation of earth resistance for a deep-driven rod in a multi-layer earth structure," *IEEE Trans. Power Del.*, vol. 6, no. 2, pp. 608–614, Apr. 1991.

[11] K. S. Bahra and R. B. Catlow, "Control of stray currents for DC traction systems," in *Proc. Int. Conf. Elect. Railways United Eur.*, Mar. 27–30, 1995, pp. 136–142.

[12] *Code of Practice for Earthing,* BS 7430, 1998.

**Charalambos A. Charalambous** (M'05) was born in Nicosia, Cyprus, in 1979. He received the Class I B.Eng. degree (Hons.) in electrical and electronic engineering and the Ph.D. degree in electrical power engineering from The University of Manchester, Manchester, U.K., in 2002 and 2005, respectively.

He is currently a Research Associate with the National Grid High Voltage Research Center, University of Manchester. His current research interests include low-frequency transformer modeling, transient studies, and the electrical control and analysis of dc corrosion.

**Ian Cotton** (M'98–SM'07) was born in the U.K. in 1974. He received the Class I B.Eng. degree (Hons.) in electrical engineering from the University of Sheffield, Sheffield, U.K., in 1995 and the Ph.D. degree in electrical engineering from The University of Manchester, Manchester, U.K., in 1998.

He is currently a Lecturer with the Electrical Energy and Power Systems Group, School of Electrical and Electronic Engineering, University of Manchester. His current research interests include power systems transients, the use of higher voltage systems in aerospace applications, and power-system-induced corrosion.

Dr. Cotton is a member of the Institution of Electrical Engineers and a Chartered Engineer.

**Pete Aylott** was born in London, U.K., in 1959. He received the M.A. degree (Hons.) in natural sciences from the University of Cambridge, Cambridge, U.K., in 1981.

Since 1985, he has been with CAPCIS Ltd., Manchester, U.K., where he is currently the Director for Infrastructure Projects. His consultancy experience covers the management of stray current on light rail and heavy rail underground systems and the interactions between these and the utility systems both across the U.K. and overseas.